**Sónia Alexandre Gouveia**

# Characterization and study of cardiorespiratory signals reciprocal relations and coupling


**Faculdade de Engenharia da Universidade do Porto**
**Faculdade de Ciências da Universidade do Porto**
**Outubro / 2004**

**Sónia Alexandre Gouveia**

# Characterization and study of cardiorespiratory signals reciprocal relations and coupling


*Tese submetida à Faculdade de Engenharia da Universidade do Porto*
*para obtenção do grau de Mestre em*
*Métodos Computacionais em Ciências e Engenharia*

Faculdade de Engenharia da Universidade do Porto
Faculdade de Ciências da Universidade do Porto
Outubro / 2004

# Abstract

The coupling between two signals is sometimes used as an index of clinical diagnosis. One example is the baroreceptor reflex sensitivity, the coupling between heart rate and systolic blood pressure, that is used as a measure of the activity of the autonomic nervous system (ANS). Respiration is an important parameter to include in this analysis. Nevertheless, its influence is largely ignored.

The main purpose of this work is the *Characterization and study of cardiorespiratory signals reciprocal relations and coupling*. In particular, to review and discuss the methodologies and algorithms for cardiovascular variability signals characterization available in the literature, for a non invasive study of the ANS. The aims of this study are to determine the relationships between oscillations in systolic blood pressure and heart rate at different breathing frequencies and to investigate other alternatives to the traditional methods.

# Resumo

A acoplagem entre dois sinais é muitas vezes utilizada como um factor de diagnóstico clínico. Um exemplo é a sensibilidade do reflexo do baroreceptor, que traduz a acoplagem entre a frequência cardíaca e a pressão arterial sistólica, e é utilizada como um indicador da actividade reflexa do sistema nervoso autónomo (SNA). A respiração é um dos factores importantes a incluir nesta análise. No entanto, é muitas vezes ignorada.

O principal objectivo deste trabalho é a *Caracterização e estudo das relações recíprocas e da acoplagem de sinais cardiorespiratórios*. Em particular, fazer uma revisão e discussão das metodologias e algoritmos para a caracterização de sinais cardiovasculares existentes na literatura, para um estudo não invasivo do SNA. São objectivos deste trabalho, o estudo das relações entre oscilações da pressão arterial sistólica e a frequência cardíaca em diferentes frequências respiratórias e a análise de outras alternativas aos métodos mais tradicionais.

# Acknowledgements

The research reported in this master thesis was carried out in Departamento de Matemática Aplicada of the Faculdade de Ciências da Universidade do Porto (DMA-FCUP).

There are lots of people I would like to thank for a huge variety of reasons.

To my supervisors, Professor Ana Paula Rocha and Professor Pedro Lago, of the DMA-FCUP, for the expert guidance, for the useful comments and for the constructive criticisms during the entire research period to the completion of this work. To Professor Pedro Lago, for his stimulating discussions and inciting ideas.

None of this work would have been possible without the dedicated experimental data provided by Philippe Van de Borne, Chef de Clinique Adjoint of the Hypertension Clinic, Department of Cardiology, Erasme Hospital, Belgium. His comments and suggestions regarding this work are gratefully acknowledged.

I would like to refer my gratitude to Centro de Estudos da Função Autonómica (CEFA), in particular to Professor António Falcão de Freitas for his inspiring research activity and his contribute to a better understanding of human autonomic (dys)functions.

For creating a pleasant working atmosphere I want to thank all of my colleagues and friends at the Departamento de Matemática Aplicada. A special thank to Rute Almeida, for her useful discussions and inputs during the development of the proposal for this work.

At last, but not the least I would like to express tremendous gratitude and appreciation to my parents, Cassiano and Otelinda, for their constant love and support throughout my entire life and for providing me the opportunity to further my education. The most special and warmest thank goes to my family Juliana and both Nunos, for their support, encouragement and understanding. They are one in a million and a million in one.

Porto, October 2004
Sónia Alexandre Gouveia

# Abbreviations

| | |
|---|---|
| ABP | Arterial Blood Pressure |
| AIC | Akaike Information Criterion |
| $\alpha$-index | Estimate of the BRS by the alpha technique |
| $\alpha^{tf}$-index | Estimate of the BRS by the transfer function method |
| ANS | Autonomic Nervous System |
| AR | AutoRegressive model |
| ARMA | AutoRegressive Moving Average model |
| BEI | Baroreflex Effectiveness Index |
| BPV | Blood Pressure Variability |
| BRS | BaroReflex Sensitivity |
| $BRS_P$ | Estimate of the BRS by the sequences technique ($P$=$\{global, local\}$ approach) |
| ECG | ElectroCardioGram |
| FFT | Fast Fourier Transform |
| HF | High Frequency band (0.15 - 0.40 Hz) |
| HRV | Heart Rate Variability |
| LF | Low Frequency band (0.04 - 0.15 Hz) |
| MSC | Magnitude Squared Coherence |
| NS | Number of Sequences |
| RESP | RESPirogram |
| RSA | Respiratory Sinus Arrhythmia |
| $r_{XX}$ | Autocorrelation function for $X$ series |
| $r_{XY}$ | Cross correlation between $X$ and $Y$ series |
| $r_{X,Y}$ | Correlation coefficient between $X$ and $Y$ series |
| $r_{X,Y\|Z}$ | Partial correlation coefficient between $X$ and $Y$ series |
| SBP | Systolic Blood Pressure |
| $S_{XX}$ | Spectrum of $X$ series |
| $S_{XY}$ | Cross spectrum between $X$ and $Y$ series |
| PSD | Power Spectrum Density |
| VLF | Very Low Frequency band (0 - 0.04 Hz) |
| $X_{seq}$ | Values of $X$ series in baroreflex sequences |

# Contents

**Appendices**

# Chapter 1

# Introduction

In this chapter, the motivation for this study is presented.
Some physiological background on cardiovascular and respiratory systems is briefly reviewed. In particular, the role of the ANS and the baroreceptor reflex for a normal heart rate regulation by blood pressure. The mechanics of respiratory activity and its interactions with cardiovascular variables are also reported.
In this chapter is also included the description of the extraction of the cardiorespiratory variability series from the original signals, with illustration.
Finally, the aims and the outline of this work are delineated.

## 1.1 Motivation

It is known that cardiovascular signals hold beat-to-beat variability. This variability reflects the interaction between the disturbances on cardiovascular variables and the regulating systems response.
It is currently accepted that heart rate variability (HRV) spectral analysis quantifies autonomic function and reflects respiratory activity (Brown *et al.*, 1993), and that the joint study of HRV and blood pressure variability (BPV) allows to access the baroreceptor reflex sensitivity (BRS) as a measure of the integrity of the ANS (Rovere, 2000). For this reason, HRV, respiration and BPV analysis and their reciprocal relations, can provide potentially important information for the interpretation of cardiovascular regulation mechanisms (Appel *et al.* (1989);Kitney *et al.* (1985)).

The interactions between HRV and BPV can be described using either *traditional techniques* or *modern techniques*.
The *traditional techniques* are invasive techniques for assessing BRS that involve the measurement of intra-arterial blood pressure and the quantification of heart rate changes when an external stimulus (such as drug infusion) is applied into the cardiovascular system.
In opposition, the *modern techniques* are noninvasive methods once they are based on instantaneous non invasive measurements of ABP (Finapres device) and do not require any external intervention. In these methods, the mutual spontaneous and simultaneous changes in blood pressure and heart rate are evaluated.

The modern techniques offer some clear advantages over traditional, namely the fact that the noninvasive nature of modern methods simplifies the test procedure, minimizes the risk, and allows the BRS measurement under a broad range of daily life conditions, making these methods more appropriate in many research settings (Watkins *et al.* (1996);Parati *et al.* (2000)).

The modern techniques can be classified into

- time domain methods (namely based in the sequences technique),
- frequency domain methods (based on cross spectral analysis and transfer function),
- or model-based approaches, either considering open or closed-loop multivariate models.

Previous comparisons between time and frequency domain methods found high levels of correlation between various techniques, but significantly different absolute values (Persson *et al.*, 2001), perhaps indicating the measurement of different physiological phenomena or even different expressions of the same. Clinical evidence show the existence of reciprocal effects, but the simplicity of open-loop models does not reflect this physiologic phenomena. Even more realistic approaches, such as closed-loop models, do not consider the specific characteristics of the two signals, assuming autoregressive models with the same order (Barbieri and Saul, 1999). For analysis methods including the respiratory information, only its potentiality is reported (Barbieri *et al.*, 1997).

Respiration is an important parameter to include in these analysis, however it is not always available. A common technique for obtaining the respiratory signal involves the measurement of thoracic impedance using the ECG electrodes and requires dedicated hardware. In its impossibility, the respiration information can be estimated from ECG signal itself (Gouveia *et al.* (2001);Rocha *et al.* (2002)). Yet, none of these methods supplies a calibrated respiration signal; only its evolution and frequency is important. With non significant amount of additional computation, any automated system for ECG and ABP analysis can use this technique to produce significant, previously unavailable information of clinical value.

For these reasons, critical reviews and improvement of existing methods, as well as the development of more realistic ones are needed, bearing in mind an accurate support to medical diagnosis.

In some frequent diseases, such as Diabetes Mellitus, one of the major complications is the autonomic nervous failure (Frattola *et al.*, 1997). In this case, persistent tachycardia and lower ABP with orthostatism, can progress to serious and incapacitating situations. The certification that HRV and BRS alterations are the earlier signs of the neurological lesions commitment (even previously than physiological, pharmacological and biochemistry methods) allow to move toward the delay of the natural evolution of the pathology and influence its own evolution. This approach can lead deeper insight into individual pattern regulation, which might allow an early detection of autonomic dysfunction at a time when intervention is still possible.

## 1.2 Physiological background

The autonomic nervous system (ANS) is responsible for the control of the internal organs (such as the heart) and of many autonomic or involuntary human body functions, such as the heart rate, blood pressure and also respiratory activity.

To accomplish this, the ANS actively identifies, integrates and interprets incoming sensory stimuli from the so called *receptors*, and produces electrochemical impulses that are distributed to generate responses to the environment and internal conditions. In this way, the receptors, which are a collection of sensory nerve endings, detect the state of the body or its surroundings and the correspondent autonomic information is transmitted.
This communication is made through the two major ANS subdivisions: the *sympathetic* and the *parasympathetic* systems. When sympathetic stimulation excites a particular organ, often parasympathetic stimulation inhibits it. That is, the two systems occasionally act reciprocally to each other, as a form a balance. For the cardiovascular control, the mutual effects of the two systems on the heart rate and on the arterial blood pressure are most significant (Robertson *et al.*, 1996).

An example of receptors are the *baroreceptors*, which are the receptors specialized to monitor changes in blood pressure. The main receptors lie in the carotid sinuses and the aortic arch; others are found in the walls of other large arteries and veins and some within the walls of the heart.
Impulses from the baroreceptors reach centers in the medulla, a part of the brain; from there autonomic activity is directed, so that the heart rate and resistance of the peripheral blood vessels can be adjusted appropriately and the necessary blood pressure is maintained. In fact, the spontaneous and automatic rhythm of the heart can be altered by ANS, and therefore both sympathetic and parasympathetic systems. Sympathetic stimulation increases the heart rate (tachycardia) and enhances the strength of heart pumping. Parasympathetic stimulation causes mainly the opposite effects: it decreases the heart rate (bradycardia) and also slightly decreases contractility.
Most blood vessels are constricted by sympathetic stimulation. Sympathetic constriction of the small arteries and the large arterioles increases the resistance and therefore reduces the blood through the vessels. Sympathetic stimulation of the veins decreases the volume of these vessels and therefore translocates the blood into the heart. Parasympathetic stimulation has little or no effect on blood vessels and it merely dilates vessels in certain restricted areas.

In this way, blood pressure is elevated by sympathetic stimulation because sympathetic activity increases propulsion of the blood by the heart and increases vessel resistance. The parasympathetic influences blood pressure in the opposite way.

The interactions between heart rate and blood pressure are regulated by means of the *baroreceptor reflex* or baroreflex, a reflex instigated by a baroreceptor. The baroreflex can be seen as a feedback in this system, as illustrated in figure 1.1, and it represents the amount of change in heart rate attributable to changes in blood pressure.
A rise in blood pressure is sensed by the baroreceptors and its reflex is stimulated. This results in a reduction of heart rate (bradycardia) and cardiac contractility and, thus, a fall in blood pressure. An initial decrease in blood pressure has opposite effects. The faster the blood pressure changes, the greater should be the baroreceptors reflex, or its sensibility to external stimulation. In this way, the baroreflex system attempts to maintain an equilibrium which helps the prevention of cardiac disturbances. In the absence or damage of arterial baroreceptors, this regulation is not possible.

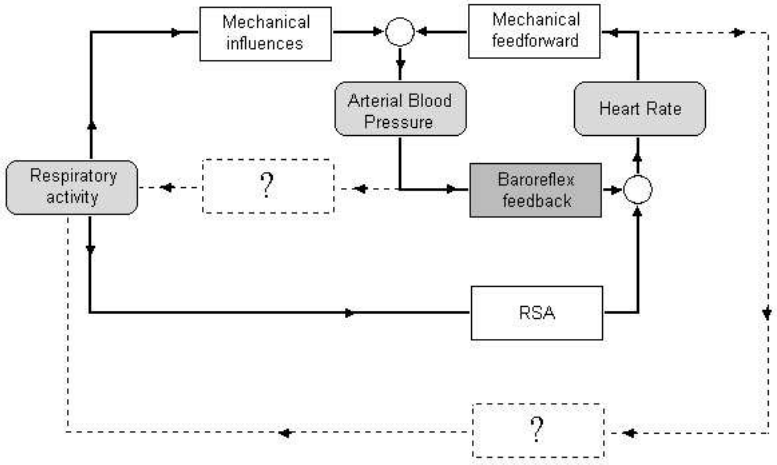


Figure 1.1: Block diagram expressing the relation between cardiorespiratory variables (dashed lines represent other possible relations (?) with unknown/unattributable physiologic meaning). Adapted from Barbieri *et al.* (1997).

Some other relations between cardiorespiratory variables are also shown in figure 1.1. In fact, heart rate and changes in heart rate are affected by many factors working in concert; including blood pressure and respiration activity.

Breathing is the only mechanism that is both autonomic and voluntary, and therefore also under the control of the ANS. The capacity of the breathing activity and the respiratory system to produce systematic variation in heart rate is referred as respira-

tory sinus arrhythmia (RSA). Typically, heart rate accelerates during inspiration and decelerates during expiration. Also, respiration exercises some mechanical influences in blood pressure.
As a closed-loop system, as blood pressure is able to determine heart rate, and therefore baroreflex sensitivity, also heart rate may influence blood pressure. Once respiratory activity is primarily under the control of the ANS, is reasonable to accept that respiration can affect both heart rate and blood pressure, and eventually the baroreflex function, performing additional coupling between the two cardiovascular variables. As they are all connected, even in case of autonomic dysfunction, breathing problems are common to occur as a direct result of loss of autonomic control.
Other relations are also accepted, although their physiological meaning is not known, as illustrated in 1.1, where the dashed lines represent other possible relations (?) with unknown/unattributable physiologic meaning.

### 1.2.1 Cardiorespiratory variability signals

Heart rate and HRV depend on multiple factors that might be simultaneously interacting, including ABP and respiration activity. For this reason, the joint analysis of such variability can provide quantitative and noninvasive measures on cardiovascular function (Appel *et al.*, 1989).

Cardiovascular variables, such as HR and ABP are almost *periodical*, although showing some variability on a beat-to-beat basis, as is illustrated in figure 1.2, with typical ECG and ABP signals. The respiration also exhibits a periodical pattern that, when compared with ECG and ABP, evidences a slower evolution.

After signal acquisition, the variability of each signal is extracted, as illustrated in figure 1.3, for ECG, ABP and respiratory signals.
From the ECG signal, the simplest series that can be used to characterize HRV is the RR interval series (or tachogram). The tachogram is defined as the time between two consecutive heartbeats and is usually measured in *sec* or *msec* units.
From the ABP signal, the consecutive systolic (or maximum) blood pressure values compose the SBP series (or systogram) and it is usually measured in *mmHg* units.
For a beat to beat respiratory pattern, the respiratory activity signal is usually sampled once every heartbeat, in correspondence with the R wave in the ECG. This procedure produces the RESP series (or respirogram), which is synchronized with the tachogram. Its amplitudes are usually in *Volt* or *mVolt* units, once the continuous signal is obtained by thoracic impedance.

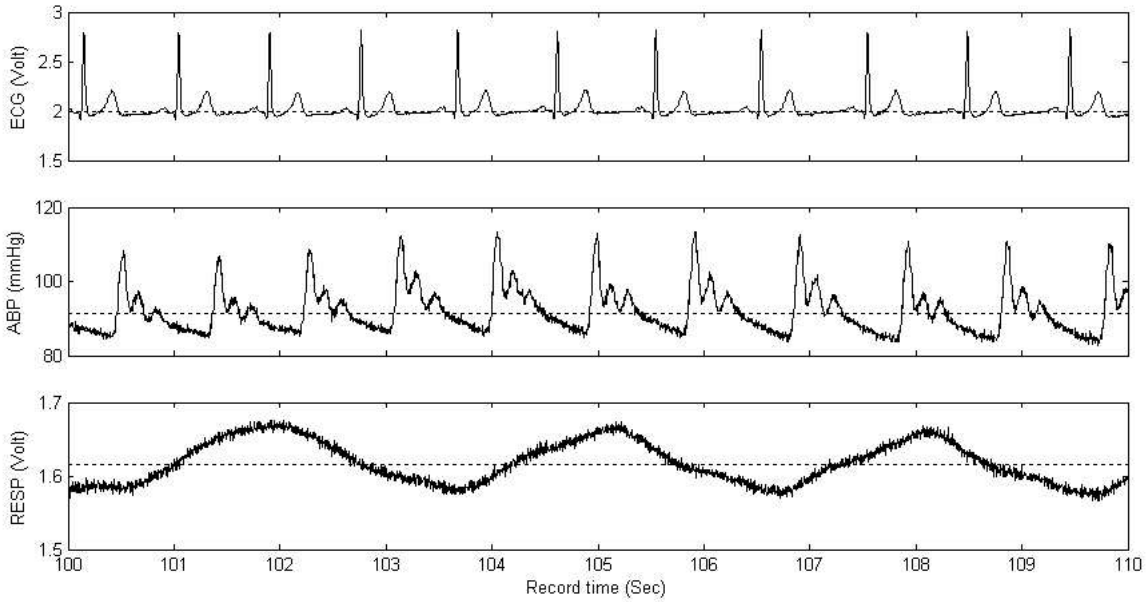


Figure 1.2: Cardiorespiratory signals. The electrocardiogram (ECG), arterial blood pressure (ABP) and respiration experimental signals. Normal subject in controlled respiration at 20 breath *per* minute.

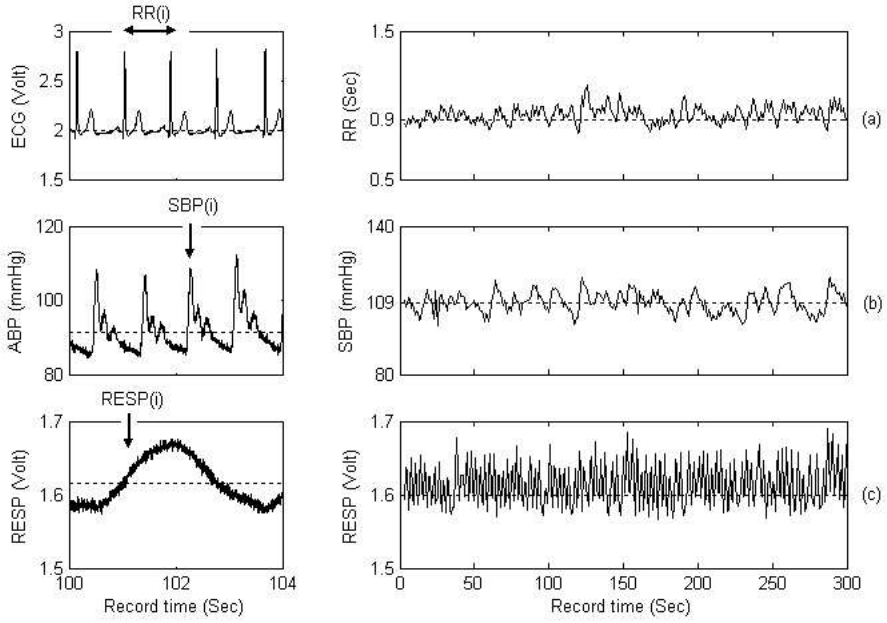


Figure 1.3: Cardiorespiratory variability series. RR is obtained after a peak detection in the ECG signal (a); SBP is obtained after peak detection in the ABP signal (b); RESP is obtained by sampling the respiration signal at a peak in the ECG (c).

## 1.3 Aims and the outline of this work

The main purpose of this work is the *Characterization and study of cardiorespiratory signals reciprocal relations and coupling*. In particular to overview, report and discuss the methodologies and algorithms for cardiorespiratory variability signals characterization available in the literature, for a non invasive study of the ANS.

An introduction and motivation for this work is presented in chapter 1. The physiology of the cardiovascular and the respiratory system is reviewed. In particular, the role of the ANS is described as well as the baroreceptor reflex and the mechanics of respiratory, and their interactions. A brief introduction to cardiorespiratory signals is also presented, including their physiological interpretation and the common ways to extract representative variability.

Chapter 2 and 3 contain a review of the most common signal analysis methods applied to cardiovascular variability signals, considering either a single signal or the combined study of cardiorespiratory variables, including time domain, frequency domain and model based analysis. The methods are illustrated with experimental data and their limits and advantages are discussed. In order to access SBP and RR mutual relations, and therefore the BRS estimative value, alternatives to the traditional methods are proposed, in order to include the respiratory information.

In chapter 4, the experimental settings are described. Also, the results are presented and discussed in the scope of their physiological meaning. The methods described and proposed in chapter 2 and 3 are evaluated and compared, when possible also including respiration.

The final chapter summarizes the results, presenting the important conclusions of this work, final considerations and some ideas for future development.

The appendices provide technical details on the methodologies presented.

# Chapter 2

# Methods for cardiovascular variability series analysis

Heart rate variability analysis has become an important tool in cardiology, because its measurements are non invasive and easy to perform, without interfering with the normal functioning of the cardiovascular control mechanisms. Also, HRV analysis can provide prognostic information on patients with different autonomic level dysfunction (Camm *et al.* (1996);Freitas (2000)).

The analysis of cardiovascular variability series provides crucial information to describe, understand and help in the diagnosis of several autonomic (dys)functions. To this purpose, both time and frequency domain methods are used.
Although the understanding of the meaning of HRV is far from complete, some standard methodologies and measures on time and frequency domain analysis are defined (Camm *et al.* (1996);Rienzo *et al.* (1999)). The variability analysis of ABP and RESP can also provide other insights or complementary perception of cardiovascular system, but a consensus for methods and measures is not established.

## 2.1 Time domain analysis

The simplest way to describe HRV, or cardiovascular variability series in general, is by means of its statistical measurements (such as common measures of location and dispersion).
In the specific case of HRV, other statistical measures can be defined, such as pNN50, the percentage of number of pairs of adjacent RR intervals differing by more than 50 ms. This measure reflects the proportion of fast increasing RR intervals in the series and can be identified as a measure of parasympathetic system activity, as it is related to high frequency information.

Another way to characterize cardiovascular series is by means of its geometric measures (Camm *et al.*, 1996). As the name suggests, the geometric measures uses the series to construct a certain geometrical form and extract some features. The histogram is used to graphically summarize and display the distribution of the values. This representation allows to study its frequency distribution and illustrate its shape, centering, and spread, indicating also whether there are any (an how much) outliers. Several measures can be extracted from the histogram, such as

- HRV triangular index: Integral of the density distribution divided by its maximum value,
- TINN: Baseline width of the distribution measured as a base of a triangle, in order to approximate the range of the series without outlier effects.

Similar statistical and geometrical measures dedicated for other cardiovascular signals (such as SBP and RESP) can also be employed, although no standard measures are reported.

## 2.2 Frequency domain analysis

Variable phenomena can be described not only as a function of time, but also as the sum of elementary oscillatory components, defined by their frequency and amplitude. The representation of this information is the so called *power spectral density* function (PSD) or *spectrum* and it describes how the variance (or power) of a time series is distributed over frequency.

The PSD function of a wide-sense stationary time series $x(n)$ with zero mean (if necessary, $x(n)$ mean is previously removed), is defined as the Fourier transform of the autocorrelation function, $r_{xx}(k)$,

$$S_{xx}(e^{jw}) = \sum_{k=-\infty}^{+\infty} r_{xx}(k)e^{-jwk}. \tag{2.1}$$

The autocorrelation function of $x(n)$ is a measure of linear dependence between $x(n)$ values at one time $n$ and the values at another time $n+k$, and is defined as

$$r_{xx}(k) = E\left[x(n)x(n+k)\right]. \tag{2.2}$$

In practice, cardiovascular series are not stationary, even eventually in wide-sense. However, short data segments may be regarded of as being locally wide-sense stationary, and PSD definition in equation (2.1) can be used.

There are several different methods for PSD estimation, that can be classified into two categories: nonparametric methods and parametric methods. In each category there are a set of methods. In this chapter, some of these methods are briefly reviewed (Manolakis *et al.*, 2000), namely

- Welch (nonparametric) and
- AR modelling from Yule-Walker equations and AIC criteria (parametric).

In cardiovascular data and in most instances, both methods provide comparable results (Costa *et al.*, 1995). This chapter will focus on these methods.

### 2.2.1 Nonparametric methods

In nonparametric methods, a usual estimator for PSD function is the Welch periodogram (Welch, 1967). The *periodogram* is defined from equation (2.1) as

$$\widehat{S}_{xx}(e^{jw}) = \sum_{n=-\infty}^{+\infty} \widehat{r}_{xx}(n)e^{-jwn} \tag{2.3}$$

where

$$\widehat{r}_{xx}(k) = \frac{1}{N}\sum_{i=1}^{N-k} x(n)x(n+k). \tag{2.4}$$

The Welch method consists in dividing $x(n)$ data into (possibly overlapping) windowed segments, computing a periodogram for each one and then averaging the estimates. If the original data is divided into $K$ segments, with $L-D$ points of overlap, each one defined as $x_i(n) = x(n+iD)$ for $n = 0, 1, ..., L-1$, the Welch estimator is given by

$$\widehat{S}_{xx}(e^{jw}) = \frac{1}{KLU}\sum_{i=0}^{K-1}\left|\sum_{n=0}^{L-1} x_i(n)w(n)e^{-jnw}\right|^2, \tag{2.5}$$

where $U$ is a normalization factor related to the window $w(n)$ characteristics

$$U = \frac{1}{L}\sum_{i=0}^{L-1} w^2(n). \tag{2.6}$$

The averaging of the periodograms leads to a consistent and asymptotically unbiased PSD estimator. Although overlap between segments tends to introduce some dependency in segments, this effect can be diminished by the use of nonrectangular windows, which reduce the importance or weight given to the end samples of segments (the samples that overlap). On other hand, the use of windowing can take in better account the specific properties of the series.
For these reasons, the overlapping between segments and the adequate window on data are two variables of the method that can be balanced in order to achieve a reduction in the PSD estimator variance and an increase in spectral resolution (Manolakis *et al.*, 2000). Alternative methods that may improve or maintain high resolution are subject of study in the next section.

Figure 2.1 illustrates the non parametric spectral analysis of an RR time series without segmentation (a) and averaging overlapping segments (Hanning window and 62,5 % of overlap). The spectral peaks presented, in VLF and LF bands and the one associated with the respiratory frequency, are more easily discerned in (b), whereas the apparent variability tends to disappear when the segmentation is introduced (b).

As the PSD estimation method assumes that discrete series $x(n)$ is wide-sense stationary, in order to introduce the time information in the frequency analysis of car-

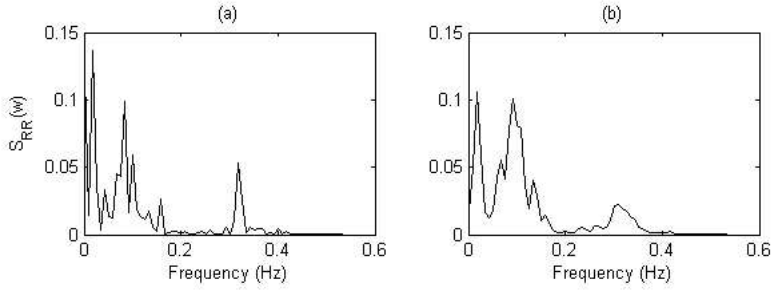


Figure 2.1: Spectral analysis of a RR time series computed with the FFT (a) without segmentation and (b) by segmentation using a Hanning window and 62,5% of overlap. Same data as in figure 1.3. Frequency axis normalized by RR mean.

diovascular data, the frequency axis in the spectra are normalized assuming a uniform sampling period equal to the mean $RR$ interval in the series.

### 2.2.2 Parametric methods

In non parametric methods, the PSD function is estimated from the signal itself. In parametric methods, the basic idea is that if a $x(n)$ series depends on a finite set of parameters, then all of its statistical properties can be expressed in terms of the model, including its autocorrelation and PSD function.
The most common and simplest of the parametric estimation techniques is autoregressive (AR) modeling of the series. The AR order $p$ model of a series $x(n)$ can be written as

$$x(n) = -\sum_{k=1}^{p} a_p(k)x(n-k) + b(0)w(n) \tag{2.7}$$

where $w(n)$ is a zero-mean stationary white noise process with unit variance. The name "autoregressive" comes from the fact that $x(n)$ is regressed on its $p$ past values, where $p$, the AR model order, represents the series memory.

The PSD function of an AR model can be estimated by

$$\widehat{S}_{xx}\left(e^{j\omega}\right) = \frac{\left|\hat{b}(0)\right|^2}{\left|1 + \sum_{k=1}^{p} \hat{a}_p(k)e^{-jk\omega}\right|^2} \tag{2.8}$$

where $\hat{a}_p(1), \hat{a}_p(2), ..., \hat{a}_p(p)$ and $\hat{b}(0)$ are the estimates of the model coefficients in (2.7). In this work, the Yule-Walker estimation technique is used, because it always produces a stable model and has simpler computational procedures (Marple, 1987).
This method of spectral estimation computes the AR parameters, by forming the biased estimate of the series autocorrelation function in equation (2.4), and solving the least squares minimization of the forward prediction error. This result in the Yule-Walker equations (2.9) that can be solved efficiently via Levinson-Durbin algorithm (Marple, 1987).

$$\hat{r}_{xx}(k) + \sum_{l=1}^{p} \hat{a}_p(l)\hat{r}_{xx}(k-l) = \left|\hat{b}(0)\right|^2 \delta(k); k \geq 0. \tag{2.9}$$

Since model order $p$ is not known a priori, the optimal model order is estimated using namely the Akaike Information Criterion (AIC) (Akaike, 1974). To obtain the optimum $p$ value, the polynomial coefficients are estimated up to a chosen maximum order and the optimum order is selected according to AIC criteria. The estimation of the AR model order is an important issue, because incorrect model orders can lead to problems of over- or under-fitting of the series.

Figure 2.2(a) illustrates the parametric spectral analysis of a RR series, computed from AR modeling, Yule-Walker equations and AIC criteria. The use of parametric methods allows a smoother spectral description of the data, than the non parametric methods (figure 2.1(b)). Also, the spectral peaks presented, in VLF and LF bands and the one associated with the respiratory frequency, are more easily discerned if the model order is adequate.

Figure 2.2(b) illustrates the zero-pole representation in the unit circle. As it is possible to observe, the poles model produce peaks in the spectrum, where sharper peaks implies poles closer to the unit circle.

### 2.2.3 Frequency domain measures

The important characteristics of the PSD function are its total power (variance) and how its power is distributed over different frequency bands, each one usually associated with a physiological meaning (Karemaker, 1997). Therefore, the decomposition of the signals variability can be achieved from the evaluation of areas in fixed frequency bands of the spectrum (typical values in table 2.1).

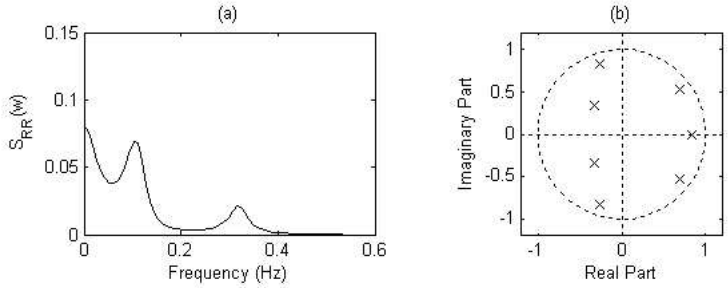


Figure 2.2: (a) Spectral analysis of a RR time series computed from AR modelling, Yule-Walker equations and AIC criteria (p=7) and (b) correspondent zero-pole representation. Same data as in figure 1.3. Frequency axis normalized by RR mean.

| Name | Frequency band (Hz) |
|---|---|
| VLF | 0-0.04 |
| LF | 0.04-0.15 |
| HF | 0.15-0.4 |

Table 2.1: Frequency bands for cardiorespiratory variability power decomposition.

Spectral analysis of the RR series, allows the identification of several components of the ANS (sympathetic and parasympathetic) and the respiratory activity. As illustrated in figure 2.3, is visible a VLF component, below 0.04 Hz, and two components associated to the LF and HF, centered approximately at 0.1 Hz and at the respiratory frequency, respectively. The decomposition of RR variability is then achieved from the evaluation of areas in the spectrum, in the fixed frequency bands in table 2.1. Parametric methods allow these components to be accurately and automatically identified from their central frequency (Zetterberg, 1969), as is illustrated in figure (b) and described in Appendix A. Similar procedures can also be applied to SBP and RESP signals.

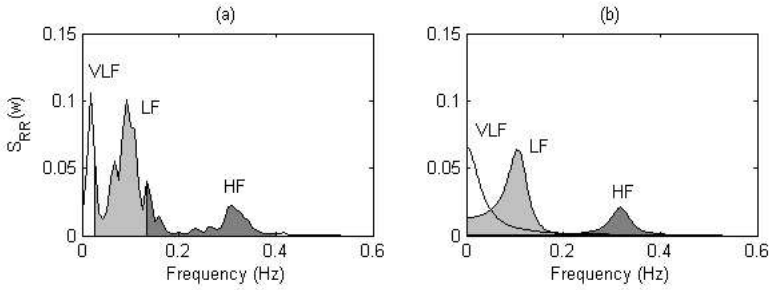


Figure 2.3: Spectral analysis of a RR time series computed with FFT (a) and from AR modelling (b) and correspondent decomposition of the spectrum in its components (b). Same data as in figure 1.3. Same methods as in figures 2.1 and 2.2, respectively. Frequency axis normalized by RR mean.

# Chapter 3

# Methods for the analysis of cardiorespiratory series interactions

A wide variety of algorithms and models have been proposed to study spontaneous cardiovascular variability interactions and to characterize the relation between the changes in RR and SBP. The optimal methods for extracting such information and the most appropriate interpretations of the results obtained are still issue of considerable debate (Parati and Rienzo, 2002), as will be discussed in this chapter. The most popular methods for BRS estimation will be presented, namely

- time domain methods (*sequences technique*),
- frequency domain methods (*alpha technique* and *transfer function*) and
- closed-loop model approaches.

## 3.1 The sequences technique

The *sequences technique* is a method for estimating the baroreflex sensitivity using time domain analysis of the spontaneous variability of SBP and RR. For this analysis, is usual to consider *sequences of consecutive beats* characterized by

- either a simultaneous increase in SBP and a lengthening in RR, also called *bradycardia* sequences,
- or a simultaneous decrease both in SBP and RR, known as *tachycardia* sequences,

as illustrated in figure 3.1 for a short segment of data.

This method is based on the assumption that changes in heart period are driven by independent changes in SBP through the baroreflex effect. These spontaneous changes constitute the *baroreflex sequences*, that correspond to the group of bradycardia and tachycardia sequences.

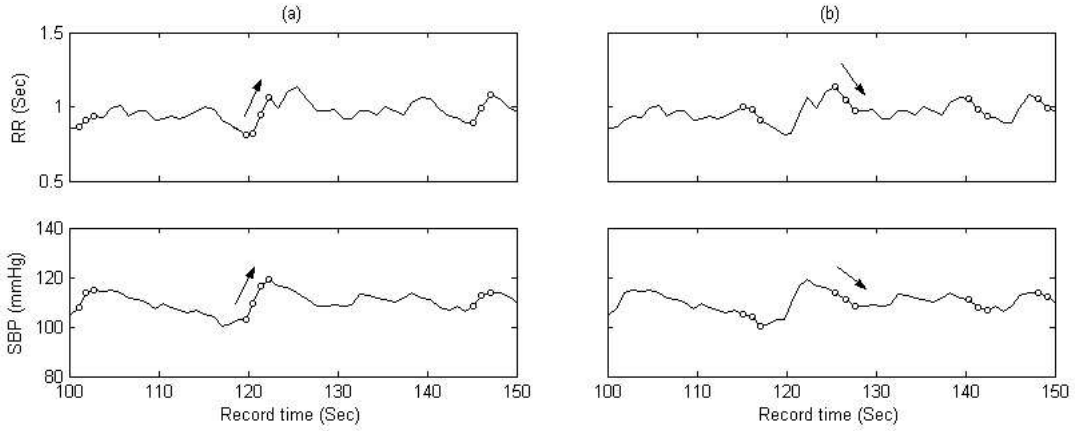


Figure 3.1: Examples of bradycardia (a) and tachycardia (b) sequences considered for BRS estimation through the *sequences technique*. Same data as in figure 1.3.

Some authors present a different notation for bradycardia and tachycardia; bradycardia sequences are also referred as *up* sequences and tachycardia as *down* sequences. In this work, the definition for up and down sequences is reserved for RESP series, where an up (or down) sequence is the name for sequences that have RESP series values in simultaneous progressive rise (or decrease) behaviour, corresponding to inspiration (or expiration) phase in the respiratory cycle.

Since a sequence is a group of consecutive beats characterized by a concomitant increase (or decrease) in both SBP and RR, adequate thresholds have to be defined, in order to identify sequences that consist in a real baroreflex effect. For a valid baroreflex sequence, the following aspects are considered

- minimum length (number of beats) of a sequence,
- minimum step-wise changes both in SBP and RR,
- correlation coefficient threshold, and
- latency.

Although a common used method, still remains with no consensus opinion about the values for these parameters, as illustrated in table 3.1. In this table are also referred the values used in this work.

| **Parameters** | **Value** | **REF** |
|---|---|---|
| **Number of beats** | **3** | (Kardos *et al.*, 2001) |
| (beats) | 4 | (Parati *et al.*, 2000) |
| | 5 | (Tank *et al.*, 2000) |
| **SBP changes** | **1** | generally accepted |
| (mmHg/beat) | | |
| **RR changes** | 4 | (Pitzalis *et al.*, 1998) |
| (msec/beat) | **5** | (Parati *et al.*, 2000) |
| | 6 | (Frattola *et al.*, 1997) |
| **Correlation** | 0.7 | (Tank *et al.*, 2000) |
| (no units) | **0.8** | (Pitzalis *et al.*, 1998) |
| | 0.85 | (Kardos *et al.*, 2001) |
| **Latency** | **0** | in this study |
| (beats) | 1-3 | (Malberg *et al.*, 2002) |

Table 3.1: Some values for the sequences technique parameters, found in the literature. The bold values indicate the parameters values used in this work.

The diversity of values found in the literature makes the results not comparable in practice. Also, it increases the need to establish reference values, in order to allow the detection of reduced baroreflex sensitivity in individual patients.

Next, some critical appraisals about these parameters are reviewed.

**Minimum length of a sequence**

A baroreflex sequence is defined by a consecutive number of SBP and RR changes. Although the agreement in the minimum length of a sequence is not consensual, as observed in table 3.1, the fact is that the sequences technique does not make the distinction in the length of the sequences itself. In fact, Paso *et al.* (2004) show that the BRS value increases progressively as the sequence length decreases, concluding that the nature and functioning of the baroreflex is a function of the length of the sequences considered.

**Minimum step-wise changes both in SBP and RR**

The minimum consistent beat-to-beat increase (or decrease) in SBP (and RR) during a valid sequence, mean that each consecutive SBP (and RR) value must change at least that threshold to be considered a real baroreflex effect.

**Correlation coefficient threshold**

In order to accept a sequence as an acceptable baroreflex event, a minimum correlation coefficient between SBP and corresponding RR values is considered. This parameter checks for the level of linear relation between the values and specifies at which threshold their correlation will be considered as significant.

**Latency**

When there is a change in SBP, there is the possibility of the existence of an unknown physiological delay before the RR changes can occur. Latency, a synonym for delay, can be interpreted as the system response speed, in this case the baroreflex associated delay. In some sense, the question of causality is presented; a positive latency means that SBP is delayed regarding to RR, in the linear relation SBP is the cause (independent variable) and RR the effect (dependent variable). The common approach found in the literature is to consider the lag where the number of sequences is maximum.

A recent study, Malberg *et al.* (2002), presents the *Dual sequence method* (DSM), which when compared with the standard sequences technique, also includes the analysis of both synchronous and shifted time series (1 to 3 delays). The authors concluded that, apparently, the analysis of delayed regulation leads to registration of additional regulatory effects.

After the choice of the parameter values, the identified $n$ baroreflex sequences can be represented in a dispersion diagram, as is illustrated in figure 3.2(a). After mean removal for each sequence, pairs of values ($SBP^k_{seq}$,$RR^k_{seq}$) associated with each baroreflex sequence are defined, as represented in figure 3.2(b).

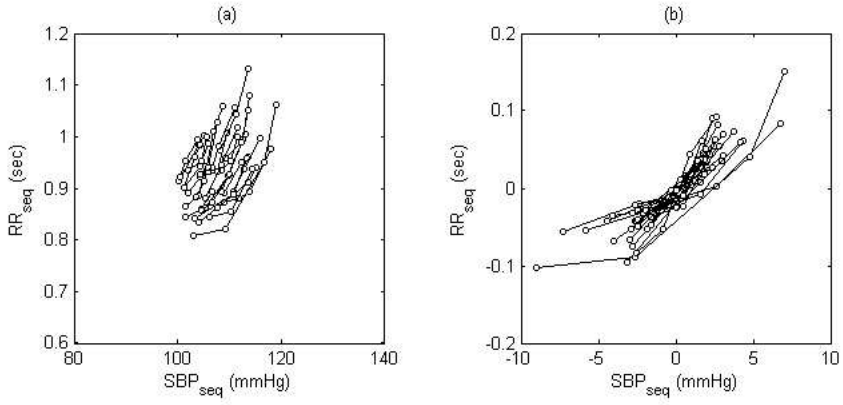


Figure 3.2: Dispersion diagram of $RR_{seq}$ and $SBP_{seq}$ values (a) and the same dispersion diagram after sequences mean removal (b). Same data as in figure 1.3.

The baroreflex effect is quantified using the following linear regression

$$RR^k_{seq} = BRS_k \, SBP^k_{seq} + c_A + \epsilon_A, \quad k = 1, 2, ...n \tag{3.1}$$

where $BRS_k$ is the quantification of BRS for the $k^{th}$ baroreflex sequence, and can be estimated by least squares. The $BRS_k$ value can be interpreted as a local measure of BRS and a natural and overall estimate can be obtained from the mean of these local estimators, as in equation 3.2. In this work, this approach is referred as *local approach*, with the correspondent $BRS_{local}$ estimator

$$BRS_{local} = \frac{1}{n} \sum_{k=1}^{n} BRS_k \tag{3.2}$$

### 3.1.1 Global approach

Least squares (LS) procedures can be strongly influenced by outliers, since a single observation can have excessive effect on the fitted model. In BRS estimation, outliers are troublesome because the estimated model should reflect globally the $n$ baroreflex sequences behavior, not just single observations.

For this reason, an alternative estimator for BRS is proposed. Instead of taking the mean of the slopes obtained for each baroreflex sequence $BRS_k$, a global measure of the baroreflex sequences is considered as the slope obtained from all the RR and SBP values, in the set of all $n$ sequences, as

$$RR_{seq} = BRS_{global}\, SBP_{seq} + c_A + \epsilon_A \tag{3.3}$$

where $BRS_{global}$ is the estimator for BRS obtained from linear regression from $RR_{seq}$ and $SBP_{seq}$, the values of RR and SBP associated with all the $n$ baroreflex sequences after mean removal. This approach will be referred as *global approach* and is illustrated in figure 3.3(b).

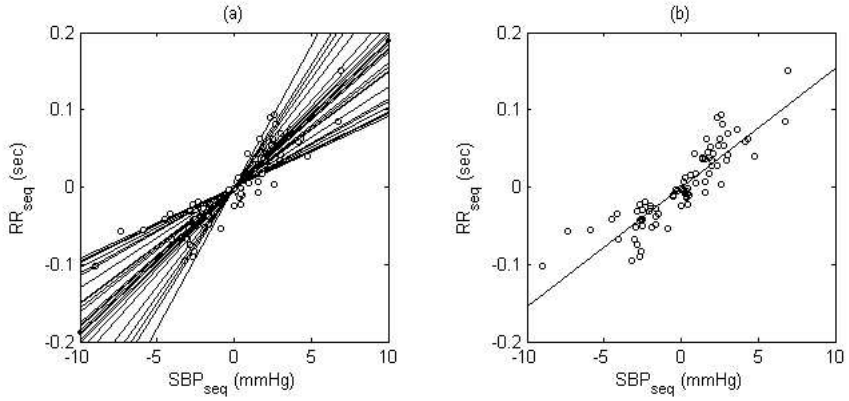


Figure 3.3: The local regression slopes (a) and the global regression slope (b), respectively local approach and global approach for the estimation of BRS. Same data as in figure 1.3.

Both local and global approaches consist in different ways of quantifying the baroreflex effect. However, the local approach can be understood as the *mean of the local baroreflex behaviour* and global approach can be interpreted as the *global mean baroreflex behaviour*.

### 3.1.2 Respiration inclusion

In this section, the inclusion of the additional information of respiration in the linear regression is discussed. Physiologically, respiration itself or even respiratory changes may influence the autonomic regulation of blood pressure and/or heart rate and eventually can activate or deactivate their coupling. The models proposed will be evaluated in chapter 4.

The global approach that describes the time relation between $RR_{seq}$ and $SBP_{seq}$ does not take into account the eventual effect of $RESP_{seq}$ and assumes the form

$$\textbf{Model A:}\ \ RR_{seq} = a_A\, SBP_{seq} + c_A + \epsilon_A \tag{3.4}$$

The simplest way to include respiratory information in the regression is to consider that both SBP and RESP information are independent variables that might explain the RR variable. In this approach, it is considered that $SBP_{seq}$ and $RESP_{seq}$ can be parallel contributions to explain $RR_{seq}$ variable, using the linear regression model

$$\textbf{Model B:}\ \ RR_{seq} = a_B\, SBP_{seq} + b_B\, RESP_{seq} + c_B + \epsilon_B \tag{3.5}$$

However, this linear formulation may not distinguish the eventual coupling between SBP and RR that can be due to the interaction of RESP with both variables, in separately. Just as the simple linear regression between $RR_{seq}$ and $SBP_{seq}$ describes their joint behavior, the two-stage regression defined as

$$\textbf{Model C:}\ \ RR_{seq} - RR_{seq}^{RESP} = a_C \left(SBP_{seq} - SBP_{seq}^{RESP}\right) + c_C + \epsilon_C \tag{3.6}$$

where $X_{seq}^{RESP}$ is the predicted value for $X_{seq}$ in the linear relation

$$X_{seq} = b_X\, RESP_{seq} + c_X + \epsilon_X, \quad X \in \{RR, SBP\} \tag{3.7}$$

allows to access the joint interactions between $RR_{seq}$ and $SBP_{seq}$, after removing the linear effect of $RESP_{seq}$ in both.

Just as the simple correlation coefficient between $RR_{seq}$ and $SBP_{seq}$ describes the RR and SBP joint behavior, the partial correlation coefficient describes the behavior of RR and SBP when the RESP linear influence is removed from both. This coefficient can be written in terms of simple correlation coefficients as

$$r_{RR_{seq},SBP_{seq}|RESP_{seq}} = \frac{r_{RR_{seq},SBP_{seq}} - r_{RR_{seq},RESP_{seq}}\, r_{SBP_{seq},RESP_{seq}}}{\sqrt{\left(1 - r^2_{RR_{seq},RESP_{seq}}\right)\left(1 - r^2_{SBP_{seq},RESP_{seq}}\right)}} \tag{3.8}$$

If RR and SBP series are both uncorrelated with RESP, from (3.8) is possible to conclude that $r_{RR_{seq},SBP_{seq}|RESP_{seq}} = r_{RR_{seq},SBP_{seq}}$. This measure corresponds to the coupling measure of RR and SBP when model C is considered.

### 3.1.3 Other time domain measures

Not every SBP ramp is invariably followed by a reflexed RR ramp, thus suggesting that in physiological conditions the baroreflex may not always be effective (Rienzo *et al.*, 2001). This can be quantified by examining the Baroreflex Effectiveness Index (BEI), that is defined as the ratio between the number of valid sequences and the overall number of SBP ramps (independent of whether these ramps were followed or not by a reflex in RR).

$$\text{BEI} = \frac{\text{total number of SBP/RR sequences}}{\text{total number of SBP ramps}} \tag{3.9}$$

This index can be seen as a measure of the efficiency of baroreflex response. The higher the BEI value, more often the baroreflex response has been excited by a sequence of changes in SBP, indicating high activity of the baroreceptor. For this reason, BEI can give information on the baroreflex function that is complementary to BRS.

## 3.2 Frequency domain methods

Cross-spectral analysis may be used to identify oscillations which have similar spectral properties, in order to investigate if the variability of two distinct series is linearly related in frequency domain. To establish this relation between SBP and RR, two methods have been proposed in the literature:

- the *alpha technique*,
- and the *transfer function method*.

These methods are based in the assumption that SBP and RR series show a high degree of linear correlation at the respiratory frequency and typically at 0.1 Hz (Camm *et al.*, 1996), and in the hypothesis that the correlation at these two frequencies is due to the baroreflex coupling. For the baroreflex function, interpreted as the capability of the cardiovascular system adjust RR to a modification in SBP, the input of the system is the SBP and its output the RR, as illustrated in the block diagram in figure 3.4.

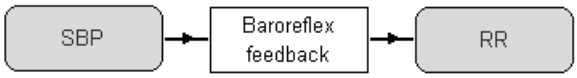


Figure 3.4: Block diagram expressing the relationship between SBP and RR in order to access baroreflex function.

Considering an input $x(n)$ and an output $y(n)$ from the system, both jointly wide-sense stationary, as was defined for autocorrelation function and spectra, their *cross-spectrum* is the Fourier transform of the crosscorrelation function $r_{xy}(k)$

$$S_{xy}(e^{jw}) = \sum_{k=-\infty}^{+\infty} r_{xy}(k)e^{-jwk} \tag{3.10}$$

The crosscorrelation function $r_{xy}(k)$ estimates the linear correlation between the series as a function of a time lag $k$ and is defined as

$$r_{xy}(k) = E\left[y(n)x(n+k)\right] \tag{3.11}$$

The cross-spectra function can be estimated using non parametric methods with segmentation (Manolakis *et al.*, 2000), identical to the Welch method described in section 2.2.1.

### 3.2.1 Significance level in coherence function

The amount of linear coupling between $x(n)$ and $y(n)$ in the frequency domain can be expressed by means of the normalized cross-spectrum, also called *coherence function*

$$k(e^{jw}) = \frac{S_{xy}(e^{jw})}{\sqrt{S_{yy}(e^{jw}) * S_{xx}(e^{jw})}} \tag{3.12}$$

The coherence, as a complex function, is usually represented by its squared magnitude (MSC) and phase separately, as illustrated in figure 3.5 for SBP and RR series.
The MSC function is a measure that is comparable to the correlation coefficient in time domain analysis, taking absolute values between zero (for frequencies where there is no coherence between series) to one (for frequencies where the series are perfectly coherent to within some fixed phase relationship) (Challis and Kitney, 1991). Under this point of view, it reflects the strength or the degree of linear correlation between the two series as a function of the frequency and phase.

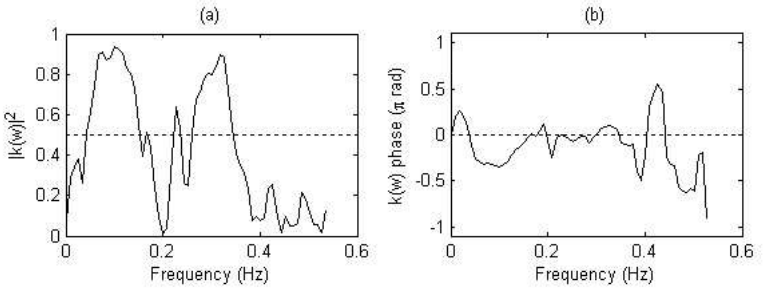


Figure 3.5: Magnitude squared coherence (a) and phase (b) between SBP and RR series, based on Welch method. Same data as in figure 1.3 and method as in figure 2.1(b). Frequency axis normalized by RR mean.

Not only to guarantee the presence of a relevant coupling between SBP and RR series, and therefore a meaningful BRS value, but also to assess a reliable transfer function estimate, a threshold level in the coherence function is usually considered, arbitrary fixed at 0.5 (Boer *et al.*, 1985).
Even so, the definition of fixed (or frequency dependent) thresholds for zero coherence is still an issue in discussion (Pinna and Maestri (2001); Faes *et al.* (2004)) and its choice becomes specially important in cases of low BRS values.

### 3.2.2 Alpha technique

The *Alpha technique* is a method for estimating the baroreflex sensitivity using frequency domain analysis of the spontaneous variability of SBP and RR.

This method is based in the assumption that SBP and RR series show a high degree of linear correlation at the respiratory frequency and typically at 0.1 Hz (Camm *et al.*, 1996), and in the hypothesis that the correlation at these two frequencies is due to the baroreflex coupling. Under these hypotheses, Robbe *et al.* (1987) proposed the $\alpha$-index for a measure of BRS, defined as the square root of ratios of SBP and RR powers in a given frequency band $B$

$$\alpha_B = \sqrt{\frac{RR_B}{SBP_B}} \tag{3.13}$$

where the coupling can be considered relevant, that is in areas where the MSC is sufficiently high, typically higher than 0.5, as discussed in section 3.2.1.

In order to distinguish baroreflex events and respiratory activity, this measure is obtained in two distinct frequency bands $B = \{LF, HF\}$, as illustrated in figure 3.6.

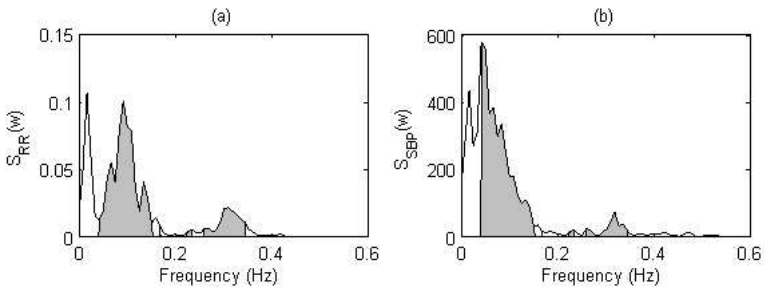


Figure 3.6: Non parametric spectra of (a) RR and (b) SBP. The gray areas show the frequency bands at which the MSC is higher than 0.5. Same data as in figure 1.3 and method as in figure 2.1(b). Frequency axis normalized by RR mean.

### 3.2.3 Transfer function method

The *Transfer function method* is a method for estimating the baroreflex sensitivity by assessing the transfer function between SBP and RR.

The transfer function is a complex-valued function of the frequency $w$ expressing the relationship between the output $y(n)$ and input $x(n)$ of a system: when the transfer function operates on $x(n)$, the $y(n)$ is obtained. For a linear system, the transfer function $H(e^{jw})$ is given by

$$H(e^{jw}) = \frac{S_{yx}(e^{jw})}{S_{xx}(e^{jw})} \tag{3.14}$$

Remembering the expression of the coherence function $k(e^{jw})$ in equation 3.12, thus

$$\left|H(e^{jw})\right|^2 = k^2(e^{jw})\frac{S_{xx}(e^{jw})}{S_{yy}(e^{jw})} \tag{3.15}$$

and a relation between the $|H(e^{jw})|^2$ and the MSC function $k^2(e^{jw})$ is established.

The magnitude and phase of the transfer function between SBP and RR is illustrated in figure 3.7. The BRS value is estimated as the mean value of transfer function magnitude that rely in the frequency bands at which the minimal coherence value is achieved, as discussed in section 3.2.1. In order to provide a comparable measure with the alpha technique, this measure is obtained in two distinct frequency bands $\alpha_B^{tf}$, $B = \{LF, HF\}$.

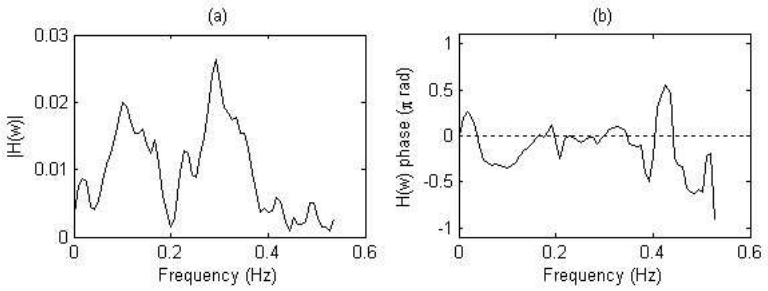


Figure 3.7: Transfer function magnitude (a) and phase between SBP and RR, based on Welch method. Same data as in figure 1.3 and method as in figure 2.1(b). Frequency axis normalized by RR mean.

## 3.3 Closed-loop model approach

The autonomic control of heart rate and blood pressure involves several feedforward and feedback mechanisms, as described in section 1.2. In addition, respiration affects both variables through mechanical mechanisms and RSA, respectively. Therefore, in order to analyze the mutual interactions between HRV and BPV and control the respiration related influences, there is the need for closed-loop approaches.

Is currently accepted that the mutual interactions between SBP and RR can be described using multivariate AR models. The *bivariate model approach* is able to consider the feedback and feedforward mechanisms between them, evaluating BRS in a closed-loop context (Barbieri and Saul, 1999). In this approach, RESP series represents an activity that affects each variable independently and therefore is not considered. These mutual relations can be illustrated in the following simplified model in figure (3.8), and can be expressed as a function of the AR coefficients estimated $A_{ij}$, with $i, j = 1, 2$.

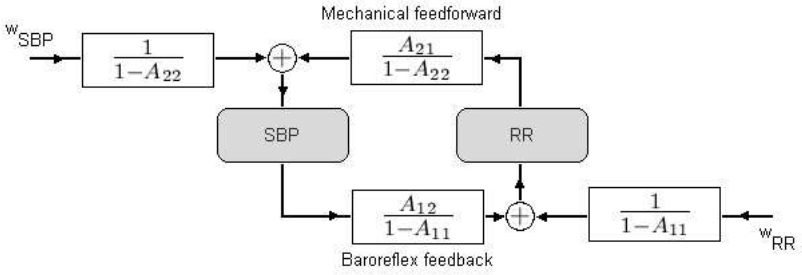


Figure 3.8: Simplified model to describe closed-loop bivariate model approach.

These assumptions correspond to the following equations

$$\begin{aligned} RR(n) &= \sum_{k=1}^{p} a_{11}(k)RR(n-k) + \sum_{k=1}^{p} a_{12}(k)SBP(n-k) + w_{RR}(n) \\ SBP(n) &= \sum_{k=1}^{p} a_{21}(k)RR(n-k) + \sum_{k=1}^{p} a_{22}(k)SBP(n-k) + w_{SBP}(n) \end{aligned} \tag{3.16}$$

where the variables are assumed to result from two uncorrelated stationary zero-mean white noises, $w_{SBP}$ and $w_{RR}$, and from their interactions and $a_{ij}$ with $i, j = 1, 2$

represent $p$ order AR models and are the coefficients of the polynomial

$$A_{ij}(e^{jw}) = \sum_{k=1}^{p} a_{ij}(k)e^{-jwk}. \tag{3.17}$$

The *trivariate model approach*, proposed by Barbieri *et al.* (1997), is a natural extension of the bivariate model approach (3.16), in which the RESP influence is also included. The model assumes that SBP, RR and RESP interact mutually, even admitting that SBP and RR affect respiration, which have an unknown/unattributable physiologic meaning, as discussed in section 1.2. The following system describes these mutual interactions

$$\begin{aligned}
RR(n) &= \sum_{k=1}^{p} a_{11}(k)RR(n-k) + \sum_{k=1}^{p} a_{12}(k)SBP(n-k) + \sum_{k=1}^{p} a_{13}(k)RESP(n-k) + w_{RR}(n) \\
SBP(n) &= \sum_{k=1}^{p} a_{21}(k)RR(n-k) + \sum_{k=1}^{p} a_{22}(k)SBP(n-k) + \sum_{k=1}^{p} a_{23}(k)RESP(n-k) + w_{SBP}(n) \\
RESP(n) &= \sum_{k=1}^{p} a_{31}(k)RR(n-k) + \sum_{k=1}^{p} a_{32}(k)SBP(n-k) + \sum_{k=1}^{p} a_{33}(k)RESP(n-k) + w_{RESP}(n)
\end{aligned} \tag{3.18}$$

After the AR models order selection and parameters identification, described in Appendix A, both bivariate and trivariate approaches are able to assess the coherence function between the series, as illustrated in figure 3.9 for bivariate model approach.

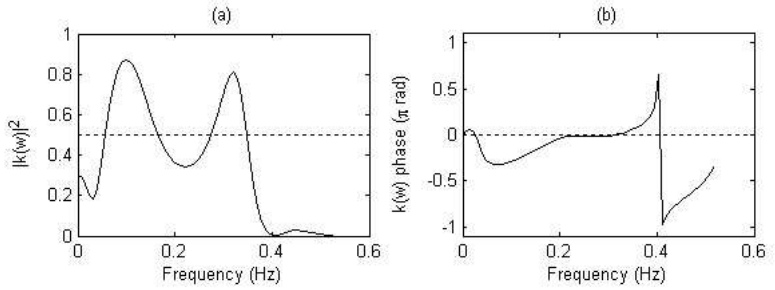


Figure 3.9: Magnitude squared coherence (a) and phase (b) between SBP and RR series, based on bivariate identification method. Same data as in figure 1.3. Frequency axis normalized by RR mean.

The definition of a coherence threshold allows to calculate some of the spectral indexes obtained with the more classical approaches, as described in section 3.2. The alpha

technique, with the BRS estimator $\alpha$-index defined as the square root of ratios of SBP and RR powers, is illustrated in figures 3.10(a) and (b). The transfer function method, with the BRS estimator $\alpha^{tf}$-index defined as the mean of the transfer function, is illustrated in figure 3.10(c).

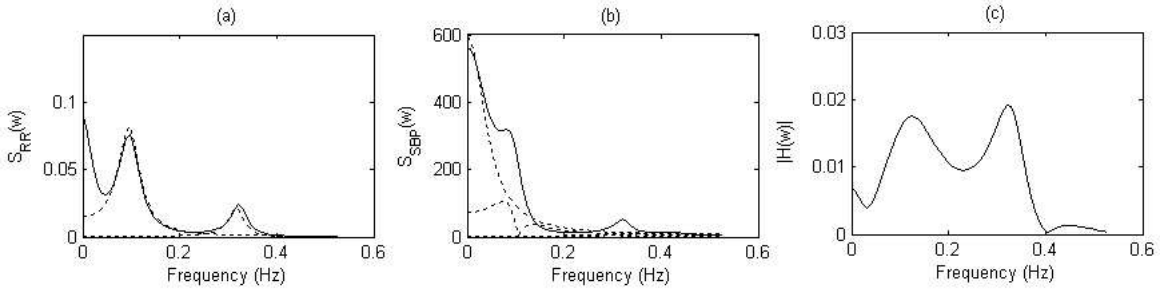


Figure 3.10: Parametric spectra of (a) RR and (b) SBP. The dotted lines represent the spectral components in the frequency bands at which the MSC is higher than 0.5. (b) Transfer function between SBP and RR series, based on bivariate identification method. Same data as in figure 1.3. Frequency axis normalized by RR mean.

The use of parametric methods allows a smoother spectral description of the data, coherence and transfer function, than the non parametric methods (figures 3.6, 3.5 and 3.7, respectively). Also, the spectral peaks presented, in VLF and LF bands and the one associated with the respiratory frequency, are more easily discerned if the model order is adequate.

## 3.4 Final considerations

The interactions between blood pressure and heart rate can be described using either *tradicional techniques* or *modern techniques*, as introduced in section 1.1.

The modern techniques are based in measures of mutual changes in blood pressure and heart rate evaluated in a spontaneous environment, do not require any external intervention. They offer some clear advantages over traditional, namely the fact that the noninvasive nature of modern methods simplifies the test procedure, minimizes the risk, and allows the BRS measurement under a broad range of daily life conditions. For these reasons, the modern techniques are more appropriate in many research settings (Watkins *et al.* (1996); Parati *et al.* (2000)).

The modern techniques can be classified bearing in mind their characteristics, as resumed in table 3.2.

| **Method** | **Brief description** |
|---|---|
| Time domain | |
| **Sequences technique**<br>Blaber *et al.* (1995)<br>Malberg *et al.* (2002) | BRS as a measure of linear relation between sequences of beats where spontaneous SBP and RR changes are coupled due to baroreflex effect |
| Frequency domain | |
| **Alpha technique**<br>Pagani *et al.* (1988) | BRS as square root of ratio between RR and SBP powers in a given frequency band |
| **Transfer function**<br>Robbe *et al.* (1987) | BRS as the mean value of the transfer function magnitude between RR and SBP in a given frequency band |
| Closed-loop model approach | |
| **Closed-loop Bivariate**<br>Barbieri and Saul (1999) | Quantification of the feedback (BRS) and the feedforward relationships between SBP and RR |
| **Closed-loop Trivariate**<br>Barbieri *et al.* (1997) | Quantification of the feedback (BRS) and the feedforward relationships between SBP, RR and RESP |
| Others | |
| **Complex Demodulation**<br>Shin and David (1997) | BRS as the ratio between SBP and RR amplitude oscillations assessed by complex demodulation |
| **Z-analysis**<br>Cerutti *et al.* (1995) | Statistical evaluation of the relationship between SBP and RR based on the calculation of the Z-coefficient |

Table 3.2: Methods for the assessment of spontaneous baroreceptor reflex sensitivity.

Previous comparisons between time and frequency domain methods found high levels of correlation between various techniques, but significantly different absolute values (Persson *et al.*, 2001), perhaps indicating the measurement of different physiological phenomena or even different expressions of the same. Clinical evidences show the existence of reciprocal effects, but the simplicity of open-loop models does not reflect this physiologic phenomena. Even more realistic approaches, such as closed-loop models, do not consider the specific characteristics of the two signals, assuming autoregressive models with the same order (Barbieri and Saul, 1999). For analysis methods including the respiratory information, only its potentiality is reported (Barbieri *et al.*, 1997).

# Chapter 4

# Results

In this chapter, the experimental settings are described.
The interactions between the cardiorespiratory variables are investigated using different approaches. The results for each experiment are presented and discussed in the scope of their physiological meaning. The methods described in chapter 3 are also evaluated and compared, when possible also including respiration. Additionally, a critical review of the several estimators for BRS value is provided.

## 4.1 Experimental settings

The experimental data used in this work consists in 68 sets of simultaneous ECG, ABP and respiratory signals from 11 young normal volunteers (10 males, 1 female), with mean age 26 years (range 19-37 years) and not taking medication. This data was already object of study in the literature (Borne *et al.*, 2000).

**Study protocol**
In each acquisition, the volunteer was asked to control his breathing, typically at frequencies 0.19, 0.27 and 0.33 Hz. The distribution of the signals sets *per* breathing frequency is illustrated in figure 4.1.

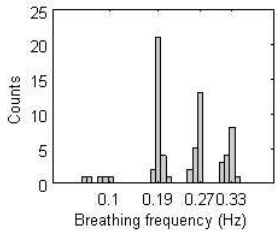


Figure 4.1: Distribution of the experimental data over breathing frequency.

**Measurement equipment**
ABP signal was measured continuously at the finger level (Finapres, Ohmeda 2300, Englewood, CO) and both ECG and respiratory signals were collected using a pneumograph and a "Gould 2800 S" recorder. The volunteers controlled their breathing with the use of a metronome throughout the experiment. Breathing was via a mouthpiece with a nose clip to ensure exclusive mouth breathing and minute ventilation was determined using a Kozak flow-volume turbine module (Vacumetrics). Analog-to-digital conversion was performed at 300 samples/s for the ECG, ABP and respiratory signals. The data were then analyzed off-line, in similar procedures as described in section 1.2.1. In this way, each data set was constituted by three cardiorespiratory variability series: RR, SBP and RESP, as illustrated in figure 1.3.

**Processing software**
All the computation involved in this work was designed to achieve a good performance in terms of timing accuracy and reliability. Also, a structured development of the methodologies and the possibility of an easy incorporation of new methods was of great interest, bearing in mind their inclusion in a friendly user interface. The algorithms have been implemented in Matlab software (The Mathworks, Inc, Natick, MA), using the methods described in chapters and 2 and 3.

## 4.2 Sequences technique methods

In this section, the traditional sequences technique is evaluated and compared with alternative proposed approaches, described in section 3.1.

A robustness analysis of the traditional estimator (local approach) is performed and a new estimator for BRS value estimation is evaluated (global approach). Considering the global approach, the possibility that simultaneous oscillations of SBP and RR could be modulated by respiration is also investigated and other linear models are suggested.

### 4.2.1 Evaluation and robustness analysis

After the identification of the baroreflex sequences, a measure of BRS can be obtained using the local or the global approach, as described in section 3.1.1.

To compare and evaluate the global versus local approach a simulation study was performed. In order to ensure a linear time relation between them and to access the reference value for BRS, uncorrelated RR series realizations were simulated using the linear model

$$RR_s = BRS_{ref}\,(SBP - \overline{SBP}_{seq}) + \overline{RR}_{seq} + \epsilon. \tag{4.1}$$

$BRS_{ref}$=0.00814 is the reference value for BRS and $\epsilon \sim N(0, \sigma^2)$ is uncorrelated zero-mean white noise with adequate $\sigma^2$ to maintain a realistic variance in $RR_s$. All the parameters of the model were extracted from a real record.

A typical estimates distribution is illustrated in figure 4.2 with the $mean \pm std(\times 10^{-3})$ values $10.514 \pm 0.68244$, for local approach and $9.4893 \pm 0.35495$ for global approach.

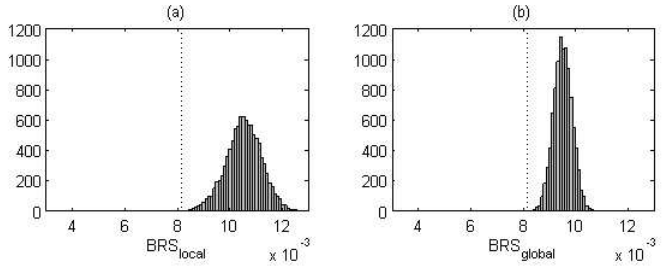


Figure 4.2: Distribution BRS estimated values using (a) local and (b) global approach (N=10000 simulations). Dotted line stands for BRS reference value.

As observed, both local and global are biased estimators but global estimator presents a relevant variance reduction. Also, the global approach has the advantage of being more efficient in computation, once it performs only a LS regression over the entire baroreflex sequences values. For these reasons, the use of the global is advantageous.

The robustness of the estimators was also compared in the presence of outliers.
Each RR series from the experimental data was perturbed in the last element of the first bradycardia sequence with a small perturbation $\epsilon_p$=0.0001, corresponding to a percentage of the minimum step-wise changes in RR series for the acceptance of a baroreflex sequence. The perturbed estimators $BRS^{(p)}_{local}$ and $BRS^{(p)}_{global}$ are deduced in appendix B and they can be written as a function of the non-perturbated estimators $BRS_{local}$ and $BRS_{global}$ plus an error of perturbation $E^{(p)}_{local}$ and $E^{(p)}_{global}$ as

$$\begin{aligned} BRS^{(p)}_{local} &= BRS_{local} + E^{(p)}_{local} \\ BRS^{(p)}_{global} &= BRS_{global} + E^{(p)}_{global} \end{aligned} \tag{4.2}$$

The respective estimates errors, $E^{(p)}_{local}$ and $E^{(p)}_{global}$, are illustrated in figure 4.3. As observed, the error introduced in the global estimator is lower than the error introduced in the local approach. Also, $E^{(p)}_{global}$ is insignificant in the estimative for BRS, while $E^{(p)}_{local}$ introduces an error in the third significative digit of BRS value.

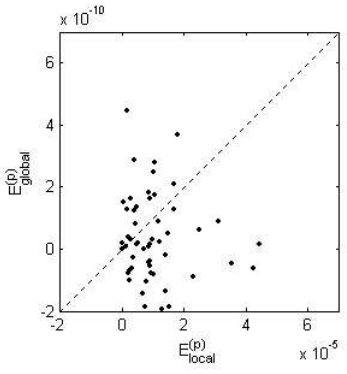


Figure 4.3: Dispersion diagram of the errors $E^{(p)}_{local}$ and $E^{(p)}_{global}$ in the estimative for BRS using local and global approaches, when a perturbation $\epsilon_p$=0.0001 is introduced in one value of one baroreflex sequence.

### 4.2.2 Respiration inclusion

In this section, the importance of the inclusion of the additional information of respiration in the linear regression is investigated, using the traditional and proposed models described in section 3.1.2. The aim is to study if respiration itself or even respiratory changes may influence the autonomic regulation of SBP and/or RR and eventually can activate or deactivate their coupling.

In order to characterize the relation between cardiovascular variables and respiratory activity, the correlation coefficient, which measures the degree of linear relation between two series, was considered. Figure 4.4 illustrates the correlation coefficients of $RR_{seq}/RESP_{seq}$ (that is, the correlation coefficient between RR and RESP in the baroreflex sequences) and $SBP_{seq}/RESP_{seq}$, showing that the degree of linear influence between $RESP_{seq}$ and $RR_{seq}$ and between $RESP_{seq}$ and $SBP_{seq}$ is identical, but not always relevant. To note that this influence is notoriously in the opposite way, that is, the correlation coefficients are mostly negative: RESP increasing (or decreasing) is related with both SBP and RR decreasing (or increasing).

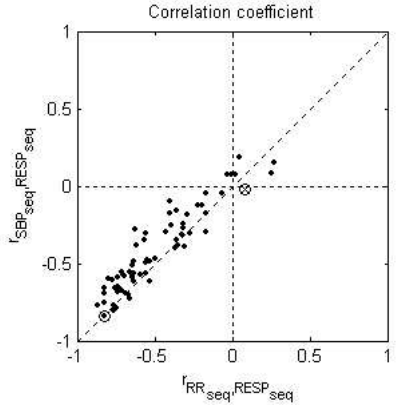


Figure 4.4: Dispersion diagram of the $RR_{seq}/RESP_{seq}$ correlation coefficient and the $SBP_{seq}/RESP_{seq}$ correlation coefficient; ($\otimes$) represents the sample data set with the lowest $RR_{seq}/RESP_{seq}$ correlation and ($\odot$) the case of highest $RR_{seq}/RESP_{seq}$ correlation.

A more detailed analysis of the extreme examples ($\otimes$) and ($\odot$) is illustrated in figure 4.5, where ($\otimes$) is the sample data set with the lowest correlation between $RR_{seq}$ and $RESP_{seq}$ and ($\odot$) the case of highest correlation between $RR_{seq}$ and $RESP_{seq}$. As it is possible to observe, in the case of highest correlation from the dispersion diagram in figure 4.4, there is the evidence that RESP variable can explain some of the RR series variability.

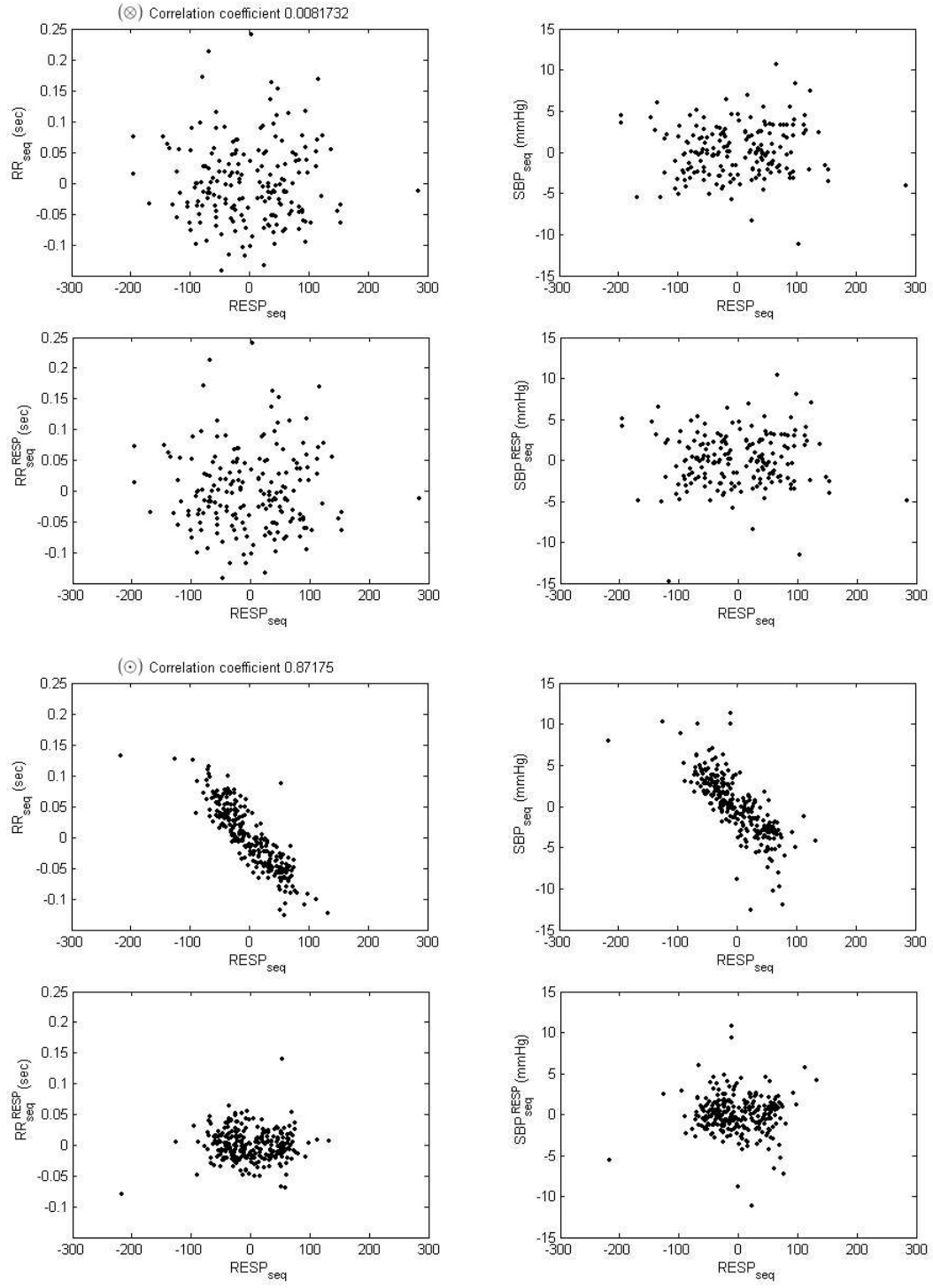


Figure 4.5: Dispersion diagrams of $RESP_{seq}$ with $RR_{seq}$, $SBP_{seq}$, $RR_{seq}^{RESP}$ and $SBP_{seq}^{RESP}$ for the baroreflex sequences in two data sets in the extreme situations. Top four graphs for ($\otimes$) the sample data set with the lowest $RR_{seq}/RESP_{seq}$ correlation and lowest four graphs for ($\odot$), the case of highest $RR_{seq}/RESP_{seq}$ correlation.

**Analysis of the models A, B and C**

In order to describe the time relation between SBP and RR, the BRS values estimated using the different models A, B and C presented in section 3.1.2, were compared.

The results obtained for each sample data set are illustrated in figure 4.6. The global approach (A) seems to overestimate the BRS estimative $a_A$, whereas the proposed models B and C give similar values, $a_B$ and $a_C$ as illustrated in figure 4.6(a). This behavior can be explained by the fact that some of the RR effects derived from SBP eventually are due to RESP, and are simultaneously present in SBP series.
For a quantitative evaluation of the models, the associated explained variance is illustrated in figure 4.6(b). Regarding model B, it is natural to observe an increase in this value. This is due to the fact that when additional variables are added to a regression equation the explained variance by the model increases, even when the new variables have no real predictive capability. The fact that the simple and partial correlation coefficients are different (respectively, values for model A and C in figure 4.6(b)), ensures that the linear relation between RR and SBP series is indirectly influenced by RESP linear effects in both cardiovascular series.

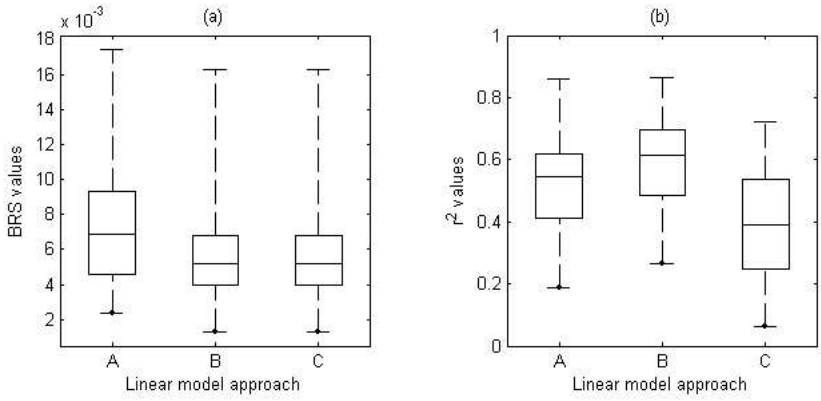


Figure 4.6: (a) BRS values for the sample data sets, and (b) associated explained variance, estimated from global approach A and two proposed models, B and C.

The relation between the $a_A$ and $a_C$ estimated values is represented in figure 4.7 (a). The global approach (A) overestimates the BRS estimative, once $a_A > a_C$ for all the sample data. For the sample data set with the lowest $RR_{seq}/RESP_{seq}$ correlation ($\otimes$), $a_A$ and $a_C$ have similar values. On the other hand, for the sample data set with the highest $RR_{seq}/RESP_{seq}$ correlation ($\odot$), the estimated parameters present the maximum difference. As a matter of fact, as illustrated in figure (b), the proportion between the two estimates is a function of the correlation degree between RESP and

the cardiovascular variables; the higher the correlation between them, the higher the difference between the estimators, where $a_A > a_C$ for all cases.

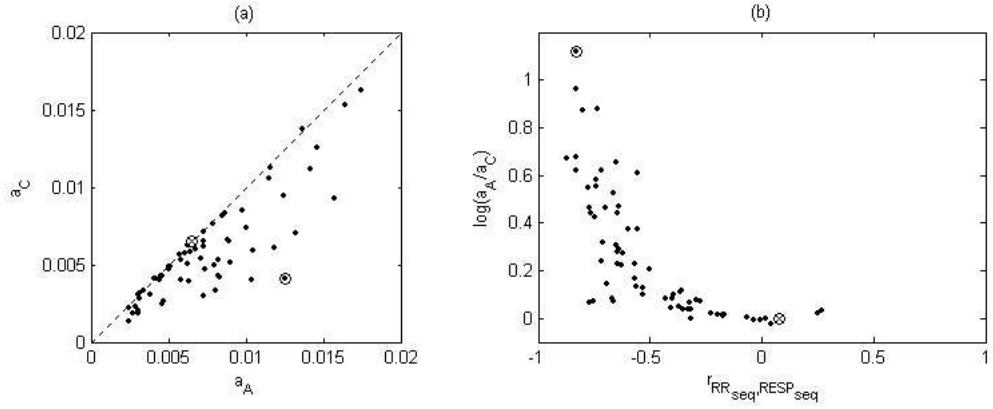


Figure 4.7: Dispersion diagram between the estimated parameters $a_A$ and $a_C$ (a) and dispersion diagram between correlation coefficient between $RR_{seq}$ and $RESP_{seq}$ and $log(a_A/a_C)$ (b), where ($\otimes$) represents the sample data set with the lowest $RR_{seq}/RESP_{seq}$ correlation and ($\odot$) the case of highest $RR_{seq}/RESP_{seq}$ correlation.

From the three models analysis, there is the strong evidence that RESP has a direct influence in both SBP and RR variables, and has indirect effects of this similar relation in the SBP and RR coupling. For this reason, it is natural to expect that the global approach to BRS assessment provides higher values, when compared to model approach C.

RESP seems to be an important variable to consider, moreover in experimental protocols that impose controlled breathing frequencies. For spontaneous respiration protocols, other studies have to be considered.

### 4.2.3 Baroreflex sequences and respiration

In this section, the timing of baroreflex sequences is associated to the phase of the breathing cycle. Also, some experiments are accomplished in order to evaluate and explore the latency in SBP and RR series and associate their relation with the breathing frequency.

The aim is to answer the question: *Does respiration have an influence in baroreflex sequences? If that influence exists, how is it perceptible?*

**Timing of baroreflex sequences and the phase of the breathing cycle**
Since the degree of RESP linear influence over RR and SBP is similar, it is reasonable to enquire if the occurrence of baroreflex sequences is related to the phase of the breathing cycle.

As illustrated in figure 4.8, there is evidence for a strong relation between the onset of baroreflex sequences and the phase of the breathing cycle. In fact, bradycardia sequences seem to be related with up/down (inspiration/expiration) and down (expiration) phases of respiration while tachycardia sequences seem to be accompanied with down/up (expiration/inspiration) and up (inspiration).
This behavior is independent of the breathing frequency, as was verified with similar analysis.

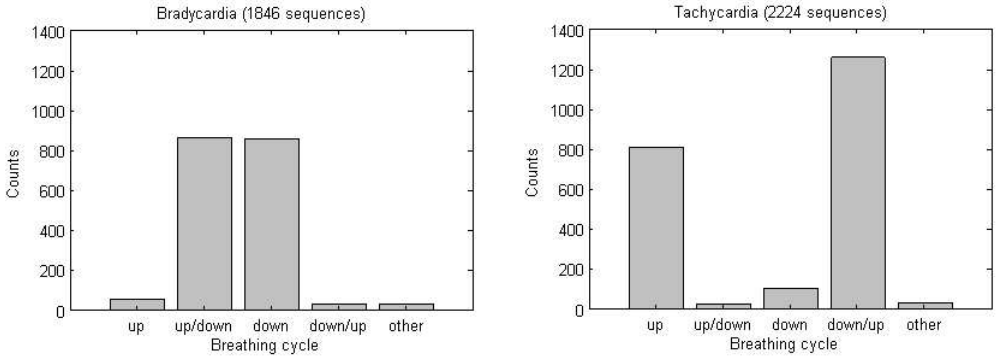


Figure 4.8: Distribution of bradycardia and tachycardia sequences over the phase of the breathing cycles: up corresponding to inspiration and down related with expiration.

This conclusion is coherent with (Rothlisberger *et al.*, 2003), that reported a strong temporal relation between the onset of baroreflex sequences and the timing from the beginning of expiration: bradycardia sequences are related with expiration and it seems that tachycardias are related with inspiration.

The association of bradycardia (or tachycardia) sequences with down (or up) respiration phase explains the negative sign of the correlation coefficient between the cardiorespiratory variables, illustrated in figure 4.4. Bradycardia sequences, that represent simulatenous increase in RR and SBP amplitudes, are associated with a simultaneous decrease in RESP, as illustrated in figure 4.9. For this reason, while the $RR_{seq}/SBP_{seq}$ simple correlation coefficient is positive (both increasing or decreasing), the $RR_{seq}/RESP_{seq}$ and $SBP_{seq}/RESP_{seq}$ is negative (decreasing or increasing).

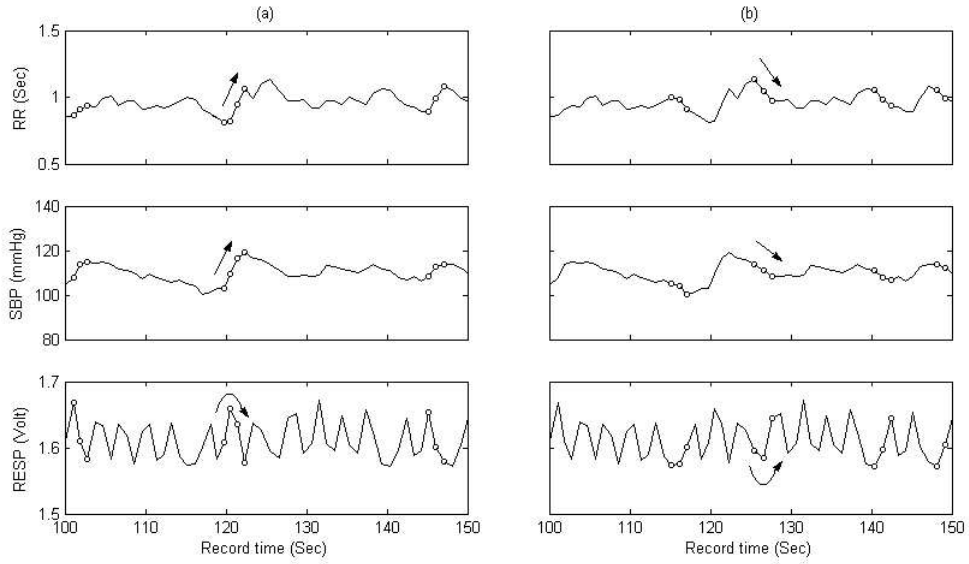


Figure 4.9: Examples of bradycardia (a) and tachycardia (b) sequences considered for BRS estimation through the sequences technique and their location in the phase of the breathing cycle. Same data as in figure 1.3.

**Number of baroreflex sequences, BEI index and latency**

The number of sequences is an important factor to be considered in the sequences technique, since a large number of sequences with a similar behavior indicate a more reliable BRS estimative, in the point of view of the estimation method. Also, the latency is a parameter that allows the sequences technique to contemplate the possibility of a delay in baroreflex response.

*Does respiration have a direct influence on the number of sequences and the latency?* To answer this question, the number of sequences (NS) was calculated by shifting RR and SBP series to a minimum latency for an appropriate PSD resolution. A periodical behavior in NS was found, as exemplified in figure 4.10 for one experimental data set. The NS fundamental frequency was automatically obtained from parametric spectral analysis, as described in section 2.2.2. The AR model order was fixed to $p = 4$, once all the NS obtained series have only one dominant frequency. In order to establish a baroreflex relation, BEI index and its frequency were calculated in the same way.

The results obtained for the experimental data are illustrated in figure 4.11. For lower respiratory frequencies (around 0.2) both NS and BEI frequencies are similar to RESP frequency but for higher frequencies, BEI and RESP frequencies are distinct.
The modulation effect of respiration in the number of frequencies is notorious, although it seems to be stronger when the individual is breathing more slowly (lower respiratory

frequencies). This means that respiration is a physiological input that can determine the number of sequences and its timing regularity. The BEI index seems to be measuring other physiological phenomena. The fact that, for lower frequencies, BEI and RESP frequency are similar may just be a coincidence. In this point, other studies have to be considered.

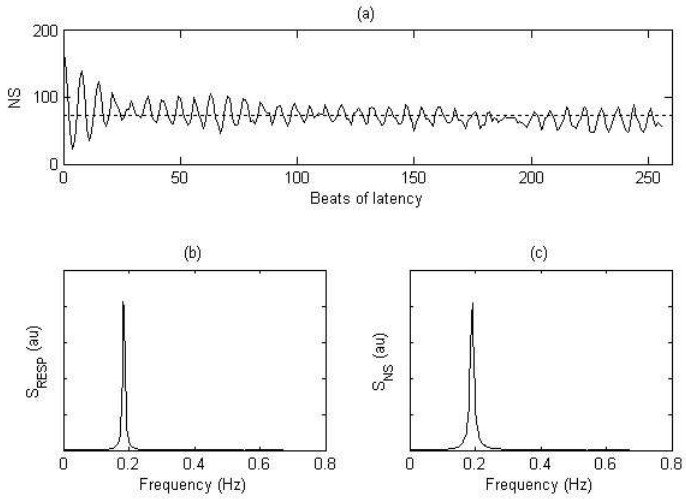


Figure 4.10: Number of sequences (NS) found by shifting RR and SBP series several beats of latency (a) for a experimental data set. Spectral analysis of RESP (b) and NS (c), using parametric spectral estimation method.

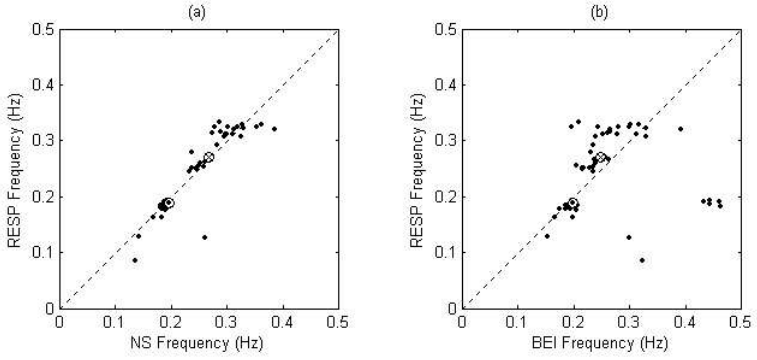


Figure 4.11: Dispersion diagrams of (a) NS and RESP frequencies and (b) BEI and RESP frequencies, where ($\otimes$) represents the sample data set with the lowest $RR_{seq}/RESP_{seq}$ correlation and ($\odot$) the case of highest $RR_{seq}/RESP_{seq}$ correlation.

## 4.3 Frequency domain methods

As described in section 3.2.1, the coherence function threshold is an important aspect to consider for the setting of frequency domain methods for BRS estimation.
The coherence function was assessed for each data set and the typical pattern is illustrated in figure 4.12 (a,b), for a respiratory frequency of 0.32 Hz, and 4.12(c,d) for a respiratory frequency of 0.19 Hz.

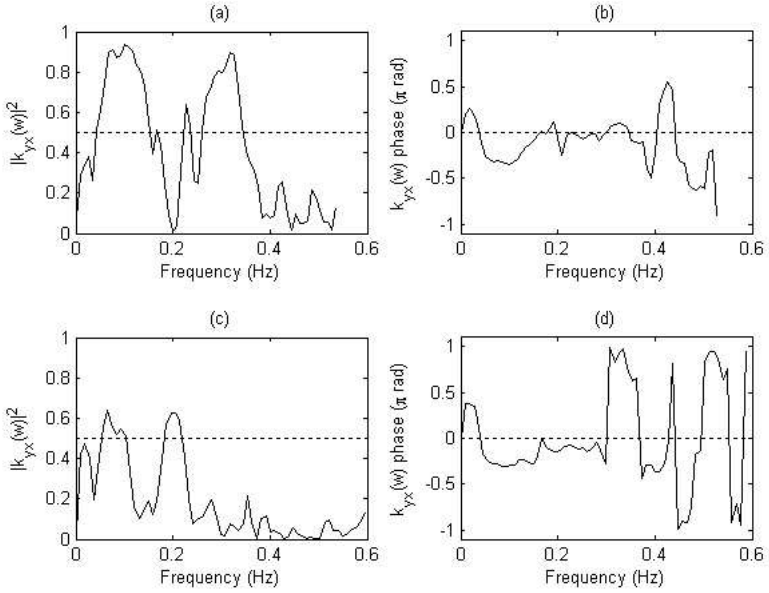


Figure 4.12: Magnitude squared coherence (a,c) and phase (b,d) between SBP and RR series, based on Welch method. Same method as in figure 2.1(b). Figures (a,b) are relative to same data as in figure 1.3 and respiratory frequency of 0.32 Hz and (c,d) to 0.19 Hz. Frequency axis normalized by RR mean.

The MSC function reflects the degree of linear relation between SBP and RR and it takes its maximum values at LF and around at the respective respiratory frequency.
The phase function indicates if the changes in the two series can or not be considered synchronous in each frequency band, allowing to access to what is the cause and the effect of the system. At LF frequency band, a negative phase is always observed, which can be interpreted as a baroreflex effect, once SBP changes induce RR changes with a determined time delay. The zero phase at HF frequency band expresses a zero time lag between the two series, indicating that their changes are synchronous. Also, it can be observed that stable phase frequencies are associated with *high* levels of coherence, eventually indicating a reliable coupling between the series.

The BRS values obtained for each frequency domain method, $\alpha_B$ for the alpha technique and $\alpha_B^{tf}$ for the transfer function method, considering each frequency band $B = \{LF, HF\}$ are compared in figure 4.13.

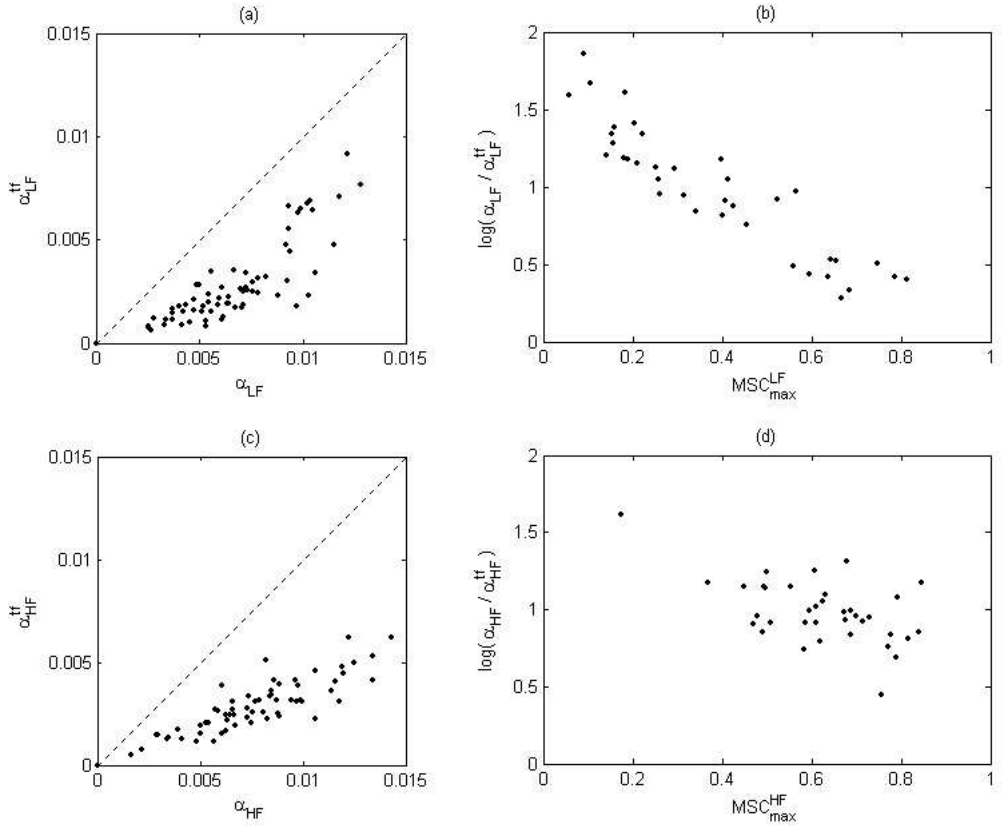


Figure 4.13: Dispersion diagram between the estimated parameters $\alpha_B$ and $\alpha_B^{tf}$ for LF (a) and HF (c) frequency bands. Dispersion diagram between the coherence maximum value and $log(\alpha_B/\alpha_B^{tf})$ for LF (b) and HF (d) frequency bands.

The relation between the estimated parameters $\alpha_B$ and $\alpha_B^{tf}$ for each frequency band $B = \{LF, HF\}$ are represented in figure 4.13 (a) and (c), respectively. Although, the estimates seem to be correlated, the alpha technique provides a higher BRS value when compared with the transfer function method, once $\alpha_B > \alpha_B^{tf}$ for all the sample data, as supported with the result obtained in Barbieri and Saul (1999).
As illustrated in figures 4.13 (b) and (d), the proportion between the two estimates is a function of the MSC maximum value; the higher the coherence between RR and SBP, the higher the resemblance between the estimates.

## 4.4 The sequences technique *vs* frequency domain methods

In this section, a comparison between sequences technique and frequency domain methods is established, in order to assess their capability to identify uncoupling between RR and SBP.

To this end, the experimental data was re-arranged in all possible combinations of pairs of sets, as described in table 4.1. Each pair of sets $A$ and $B$ was analysed separatelly. Also, from each original pair artificial series were created. The sets $A$ and $B$ were combined in $AB$ and $BA$, corresponding to RR from set $A$ and SBP from set $B$, and vice versa. To avoid the inter-variability within each subject, artificial sets such as $AC$ were produced with the division of the RR series from set $A$ in two blocks of equal size and then switched, keeping the SBP series from set $A$.

| **Combination** | **Description** |
|---|---|
| $AA$ | RR and SBP from set $A$ |
| $BB$ | RR and SBP from set $B$ |
| $AB$ | RR from set $A$ and SBP from set $B$ |
| $BA$ | RR from set $B$ and SBP from set $A$ |
| $AC$ | RR from set $A$ is divided in two blocks and these blocks are switched |
| $BC$ | RR from set $B$ is divided in two blocks and these blocks are switched |

Table 4.1: Real and artificial data used for a comparison between sequences technique and frequency domain methods.

In frequency domain methods, is usual to calculate a BRS value considering only the frequency band where the coherence between SBP and RR is significant, case in which is possible to consider that these two series are significantly coupled, as discussed in section 3.2. For this reason, the BRS value obtained with the sequences technique was studied and compared with the area of the MSC function above 0.5.

The results are illustrated in figure 4.14. As is possible to observe, the BRS values obtained by the sequences technique are similar both for real and artificial sets. However, in the artificial sets the frequency domain coupling was destroyed once the MSC area was much lower and the area above 0.5 was zero in almost all of the cases. In figure (c), the non zero areas are related with residual amplitudes in both spectra

(due to computational errors) that lead to high levels of coherence, even when the two series are evidently not coupled.

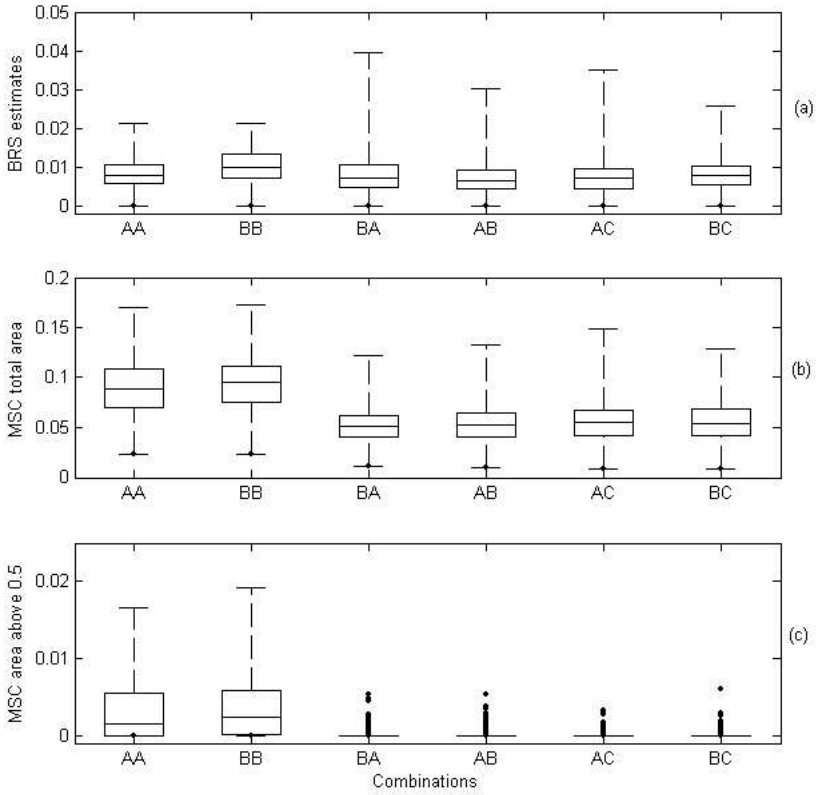


Figure 4.14: Comparison between the sequences technique and frequency domain methods: BRS value obtained by sequences technique (a), MSC total area (b) and MSC area above 0.5 (c).

These results reveal that *the sequences technique produces a estimate for BRS value, even in artificial series. Moreover, the value is comparable with the one obtained with real data.* Regarding the frequency domain methods, the area of the MSC function seems to be an important feature to consider in these methods, once it can distinguish between coupled and uncoupled pairs.

## 4.5 Model-based approach

As described in section 1.2, respiration affects both SBP and RR variables through mechanical mechanisms and RSA, respectively. Therefore, in order to analyze their mutual interactions and control the respiration related influences, there is the need for closed-loop approaches.

In this section, the bivariate and trivariate closed-loop model approaches described in section 3.3 are compared. After the models identification, as described in the appendix A, from equation (A.10) it is possible to see that each spectra can be decomposed in a sum of partial spectra, each one of these derived from the different sources. That is, it is possible to separate RR series variability into a component mediated by SBP series (due to baroreflex effect) and one component mediated by RESP series coupling (RSA), as is illustrated in figures 4.15 (for bivariate) and 4.16 (for trivariate) for an experimental data set.

As is possible to observe from 4.15, for bivariate model approach, the RR series dominant frequency in LF frequency band (around 0.1 Hz) can be explained by a larger contribution of RR series and a smaller by SBP series. For HF dominant frequency (around the respiratory frequency 0.32 Hz), the information is all due to RR and the SBP influence does not exist.

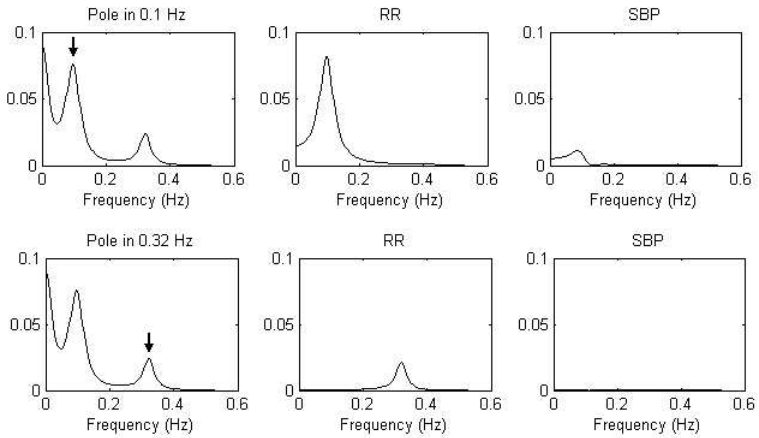


Figure 4.15: Spectral analysis of a RR series computed with bivariate AR modeling (left figures) and correspondent decomposition of each spectrum dominant frequency in its components derived from RR (middle figures) and SBP (right figures). Same data as in figure 1.3 and same methods as in figure 3.9. Frequency axis normalized by RR mean.

For trivariate model approach, as illustrated in figure 4.16, the RR series variability is decomposed in components associated with RR, SBP and RESP. In LF frequency band, the large amount of variability is explained by RR, although SBP and RESP present visible components. However, in this case, respiration seems to have more influence than SBP. In HF frequency band, the RR variability is all explained by RESP series, concluding that the RESP and RR series are coupled, eventually RESP influencing RR if the question of causality is defined.

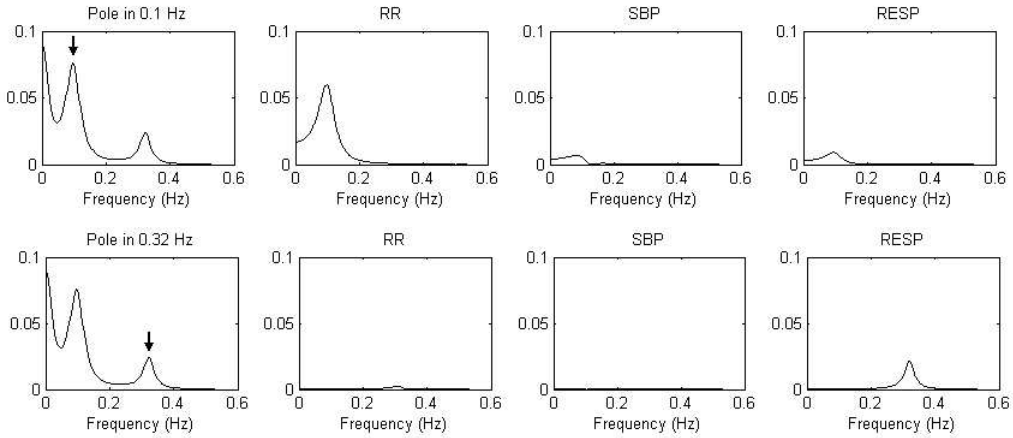


Figure 4.16: Spectral analysis of a RR series computed with trivariate AR modeling (left figures) and correspondent decomposition of each spectrum dominant frequency in its components derived from RR (middle figures), SBP and RESP (right figures). Same data as in figure 1.3. Frequency axis normalized by RR mean.

# Chapter 5

# Conclusions and Future developments

The aims of this work were to determine the relationships between oscillations in systolic blood pressure (SBP) and heart rate (RR), considering different breathing frequencies and to investigate the role of baroreflex in this relationship.
The main result is the finding that different breathing frequencies are capable of modifying these relationships. *Moreover, respiratory and respiratory frequency seems to play a major role in the time and frequency dependent phenomenon of baroreflex control, as a direct influence on both SBP and RR and an indirect influence on the relation between them.*

Although a common used method, the *Sequences technique* impose the setting of several parameters to determine what is a *valid* baroreflex event and no consensual opinion about these parameters is found in the literature. Even the methodology itself can be questionable; the estimator has not been clearly examined regarding its statistical properties (bias and variance) and robustness to outliers. The theory is sometimes overlooked, and linear regression over three values is the usual procedure. In this work, *a new estimator has been evaluated* (global approach) and it was found to be as biased as the one obtained with the traditional approach, but having lower variance distribution and more robust to outlier effects. Regarding the respiratory information, it seems to be an important variable to *look at*, moreover in experimental protocols that impose controlled breathing frequencies. Two strategies were compared to the global approach and was found clearly the advantages of respiration inclusion. For spontaneous respiration protocols, other studies have to be considered.

The frequency domain methods, *Alpha technique* and *Transfer function method* assume a strong linear relation between SBP and RR in frequency domain (high magnitude squared coherence (MSC)), but do not consider the (eventual) delay between them, nor feedback/feedforward interactions and RESP information. In this work, the frequency domain BRS estimates were compared and it was found a high level of correlation. However, the alpha technique gives a higher estimate for the BRS value and the degree of similarity between them depends on the MSC value; the higher the MSC value, the higher the resemblance between the estimates.

The comparison between the sequences technique and the frequency domain methods confirmed that *the sequences technique produces an estimate for BRS value, even in artificial series. Moreover, the value is comparable with the one obtained with real data.* This result raises the question: *what is the sequences technique really measuring?*. Regarding the frequency domain methods, the area of the MSC function seems to be an important feature to consider in these methods, once it can distinguish between coupled and uncoupled pairs.

The *Model-based approach* tries to describe mutual interactions between SBP and RR using (or not) the RESP information, but assumes the same model structure, the same order and the same delay for all signals. Although providing symmetric measures of interrelation between the series, both bivariate and trivariate approaches do not allow one to address the question of causality in the interaction between the variables. The setting of different models in the model based approach can allow to accomplish more realistic results (Nollo *et al.*, 2001).

Previous comparisons between time and frequency methods found high levels of correlation, but significantly different absolute values (Persson *et al.*, 2001), perhaps indicating the measurement of different physiological phenomena or even different expressions of the same. From this work, the resulting BRS estimative evidently depends on the method used. Moreover, the recent studies only compare the statistical results and do not analyze how and why to use some of these methods. Due to the lack of a clear methodology for autonomic measurement and the lack of consistency in analysis of the methods, reference values for both healthy and pathological individuals have not been established. For these reasons, the *Characterization and study of cardiorespiratory signals reciprocal relations and coupling* is still *matter of debate* (Laude *et al.*, 2004). Without the exact definition what the measured parameter should be and its gold standard, it is difficult to discuss different analysis algorithms. But still, critical reviews and improvement of existing methods are still needed, bearing in mind an accurate support to medical diagnosis.

# References


Akaike, H. (1974). A new look at the statistical model identification. *IEEE Trans Autom Contr* **AC-19**, 716–23.

Appel, M., R. Berger and S. Saul et al (1989). Beat to beat variability in cardiovascular variables: noise or music. *J Am Coll Cardiol* **14**(5), 1139–48.

Barbieri, R., A. Bianchi and J. Triedman et al (1997). Model dependency of multivariate autoregressive spectral analysis. *IEEE Eng Med Biol Mag* **16**(5), 74–85.

Barbieri, R. and J. Saul (1999). Autoregressive modeling for assessing closed-loop feedback and feedforward in arterial baroreflex. In: *Methodology and clinical applications of blood pressure and heart rate* (M. Di Rienzo, G. Mancia, G. Parati, A. Pedotti and A. Zanchetti, Eds.). pp. 21–34. IOS Press.

Baselli, G., A. Porta, O. Rimoldi and et al (1997). Spectral decomposition in multichannel recordings based on multivariate parametric identification. *IEEE Trans Biomed Eng* **44**(11), 1092–101.

Blaber, A., Y. Yamamoto and R. Hughson et al (1995). Methodology of spontaneous baroreflex relationship assessed by surrogate data analysis. *Am J Physiol* **268**(4), H1682–7.

Boer, R. De, J. Karemaker and J. Strackee (1985). Relationships between short-term blood-pressure fluctuations and heart-rate variability in resting subjects. a spectral analysis approach. *Med Biol Eng Comput* **23**(4), 352–8.

Borne, P. Van De, S. Mezzetti, N. Montano, K. Narkiewicz, J. Degaute and V. Somers (2000). Hyperventilation alters arterial baroreflex control of heart rate and muscle sympathetic nerve activity. *Am J Physiol Heart Circ Physiol* **279**(2), H536–41.

Brown, T., L. Beighthol and J. Koh et al (1993). Important influence of respiration on human r-r interval power spectra is largely ignored. *J Appl Physiol* **75**(5), 2310–7.

Camm, J., M. Malik and J. Bigger et al (1996). Heart rate variability: standards of measurement, physiological interpretation and clinical use. task force of the european

society of cardiology and the north american society of pacing and electrophysiology. *Circulation* **93**(5), 1043–65.

Cerutti, C., M. Ducher and P. Lantelme et al (1995). Assessment of spontaneous baroreflex sensitivity in rats a new method using the concept of statistical dependence. *Am J Physiol Regul Integr Comp Physiol* **268**(2), R382–8.

Challis, R. and R. Kitney (1991). Biomedical signal processing (in four parts). part 3. the power spectrum and coherence function.. *Med Biol Eng Comput* **29**(3), 225–41.

Costa, O., P. Lago and A. Rocha et al (1995). The spectral analysis of heart rate variability: a comparative study between nonparametric and parametric spectral analysis in short series. *Rev Port Cardiol* **14**(9), 621–6. Portuguese.

Faes, L., G. Pinna, A. Porta, R. Maestri and G. Nollo (2004). Surrogate data analysis for assessing the significance of the coherence function. *IEEE Trans Biomed Eng* **51**(7), 1156–66.

Frattola, A., G. Parati and P. Gamba et al (1997). Time and frequency domain estimates of spontaneous baroreflex sensitivity provide early detection of autonomic dysfunction in diabetes mellitus. *Diabetologia* **40**, 1470–5.

Freitas, A. Falcão (2000). Cardiovascular regulation by the autonomic nervous system: a paradigm of self-organization, complexity and chaos. *Rev Port Cardiol* **19**(2), 161–91.

Gouveia, S., A. Rocha, A. Leite, P. Lago, O. Costa and A. Freitas (2001). Matlab implementation of a method for the estimation of the respiratory signal in 24-hour holter recordings. In: *BioEng - 6th Portuguese Conference on Biomedical Engineering.*

Johnsen, S. and N. Andersen (1978). On power estimation in maximum entropy spectral analysis. *Geophysics* **43**(4), 681–690.

Kardos, A., G. Watterich and R. Menezes et al (2001). Determinants of spontaneous baroreflex sensitivity in a healthy working population. *Hypertension* **37**, 911–6.

Karemaker, J. (1997). *Analysis of blood pressure and heart rate variability, Clinical Autonomic Disorders 2nd ed.* Lippincot-Raven Publishers, Philadelphia.

Kitney, R., T. Fulton and A. McDonald et al (1985). Transient interactions between blood pressure, respiration and heart rate in man. *J Biomed Eng* **7**(3), 217–24.

Laude, D., J. Elghozi and A. Girard et al (2004). Comparison of various techniques used to estimate spontaneous baroreflex sensitivity (the eurobavar study). *Am J Physiol Regul Integr Comp Physiol* **286**, R226–31.

Malberg, H., N. Wessel and A. Hasart et al (2002). Advanced analysis of spontaneous baroreflex sensitivity, blood pressure and heart rate variability in patients with dilated cardiomyopathy. *Clin Sci (Lond)* **102**, 465–473.

Manolakis, D., V. Ingle and S. Kogon (2000). *Statistical and Adaptive Signal Processing: Spectral Estimation, Signal Modeling, Adaptive Filtering and Array Processing*. McGraw-Hill Education.

Marple, L. (1987). *Digital spectral analysis with applications*. Prentice Hall.

Nollo, H., N. Wessel and A. Hasart et al (2001). Causal linear parametric model for baroreflex gain assessment in patients with recent myocardial infarction. *Am J Physiol Heart Circ Physiol* **208**, H1830–39.

Pagani, M., V. Somers and R. Furlan et al (1988). Changes in autonomic regulation induced by physical training in mild hypertension. *Hypertension* **12**(6), 600–10.

Parati, G. and M. Di Rienzo (2002). Assessing spontaneous baroreflex function: methodological considerations. *Clin Sci (Lond)* **103**(1), 89–91.

Parati, G., M. Di Rienzo and G. Mancia (2000). How to measure baroreflex sensitivity: from the cardiovascular laboratory to daily life. *J Hypertens* **18**(1), 7–19.

Paso, G. Reyes, J. Hernández and M. González (2004). Differential analysis in the time domain of the baroreceptor cardiac reflex sensitivity as a function of sequence length. *Psychophysiology* **41**(3), 483–488.

Persson, P., M. Di Rienzo and P. Castiglioni et al (2001). Time versus frequency domain techniques for assessing baroreflex sensitivity. *J Hypertens* **19**(10), 1699–705.

Pinna, G. and R. Maestri (2001). Reliability of transfer function estimates in cardiovascular variability analysis. *Med Biol Eng Comput* **39**(3), 338–47.

Pitzalis, M., F. Mastropasqua and A. Passantino et al (1998). Comparison between noninvasive indices of baroreceptor sensitivity and the phenylephrine method in post-myocardial infarction patients. *Circulation* **97**, 1362–7.

Rienzo, M. Di, G. Mancia, G. Parati, A. Pedotti and A. Zanchetti (1999). *Methodology and clinical applications of blood pressure and heart rate analysis*. IOS Press.

Rienzo, M. Di, G. Parati and P. Castiglioni et al (2001). Baroreflex effectiveness index: an additional measure of baroreflex control of heart rate in daily life. *Am J Physiol Regul Integr Comp Physiol* **280**(3), R744–51.

Robbe, H., L. Mulder and H. Ruddel et al (1987). Assessment of baroreceptor reflex sensitivity by means of spectral analysis. *Hypertension* **10**(5), 538–43.

Robertson, D., P. Low and R. Polinsky (1996). *Primer on the Autonomic Nervous System*. Academic Press.

Rocha, A., S. Gouveia, A. Leite, P. Lago, O. Costa, A. Freitas and M. Carvalho (2002). A study on the estimation of the respiratory signal in 12-lead holter recordings. In: *EMBEC'02 - 2nd Medical and Biological Engineering Conference*. IFMBE, the International Federation for Medical and Biological Engineering. pp. 508–509.

Rothlisberger, B., L. Badra, J. Hoag, W. Cooke, T. Kuusela, K. Tahvanainen and D. Eckberg (2003). Spontaneous baroreflex sequences occur as deterministic functions of breathing phase. *Clin Physiol Funct Imaging* **23**, 307–313.

Rovere, La (2000). *Methods to assess baroreflex sensitivity as a measure of the activity of the autonomic nervous system (M. Hans-H. Osterhues et al, Advances in noninvasive electrocardiograph monitoring techniques)*. Kluwer Academic Publishers.

Shin, Y. and E. David (1997). Baroreflex sensitivity assessed by complex demodulation of cardiovascular variability. *Hypertension* **29**(5), 1119–25.

Tank, J., R. Baesvski and A. Fender et al (2000). Reference values of indices of spontaneous baroreceptor reflex sensitivity. *Am J Hypertens* **13**(3), 268–75.

Waele, S. and P. Broersen (2003). Order selection for vector autoregressive models. *IEEE Trans Signal Proc* **51**(2), 427–433.

Watkins, L., P. Grossman and A. Sherwood (1996). Noninvasive assessment of baroreflex control in borderline hypertension. comparison with the phenylephrine method. *Hypertension* **28**(2), 238–43.

Welch, P. (1967). The use of fast fourier transform for the estimation of power spectra: A method based on time averaging over short, modified periodograms. *IEEE Trans Audio Electroacoust* **AU-15**, 70–3.

Zetterberg, L. (1969). Estimation parameter of a linear difference equation with application to eeg analysis. *Math Biosci* **5**, 227–75.

# Appendix A

# Multivariate AR modeling

A multivariate $\mathrm{AR}_p$ process between the $N$-observations time series $X_1$, $X_2$, ... $X_m$ is usually used to describe their mutual interactions and/or dependencies. It can be generalized from the bivariate AR model included in Barbieri and Saul (1999) and can be written as

$$\begin{aligned}
X_1(n) &= -\sum_{k=1}^{p} a_{11}(k)X_1(n-k) - \sum_{k=1}^{p} a_{12}(k)X_2(n-k) - ... - \sum_{k=1}^{p} a_{1m}(k)X_m(n-k) + W_1(n) \\
X_2(n) &= -\sum_{k=1}^{p} a_{21}(k)X_1(n-k) - \sum_{k=1}^{p} a_{22}(k)X_2(n-k) - ... - \sum_{k=1}^{p} a_{2m}(k)X_m(n-k) + W_2(n) \\
&\vdots \\
X_m(n) &= -\sum_{k=1}^{p} a_{m1}(k)X_1(n-k) - \sum_{k=1}^{p} a_{m2}(k)X_2(n-k) - ... - \sum_{k=1}^{p} a_{mm}(k)X_m(n-k) + W_m(n)
\end{aligned}$$

where $W_1(n)$, $W_2(n)$, ... $W_m(n)$ are uncorrelated stationary zero-mean white noises with variances $\lambda_1^2$, $\lambda_2^2$, ... $\lambda_m^2$ and covariances $\lambda_{j,l}^2 = \lambda_{l,j}^2 = 0$ arranged in a covariance matrix $\mathbf{\Sigma}$.

This approach considers that the present value of $X_i(n)$ is predicted by the past value of all time series involved and by the residual $W_i(n)$. The present value of each disturbance $W_i(n)$ affects directly the present value of the corresponding time series $X_i(n)$ without any delay.

## A.1 Model identification and order selection

Considering the following polynomials in the delay operator $z^{-1}$

$$A_{il}(z) = a_{il}(1)\, z^{-1} + a_{il}(2)\, z^{-2} + \cdots + a_{il}(p)\, z^{-p} = \sum_{k=1}^{p} a_{il}(k) z^{-k},\ i, l = 1, 2, ...m$$

and

$$\mathbf{A}(z) = \begin{bmatrix} A_{11}(z) & A_{12}(z) & \cdots & A_{1m}(z) \\ A_{21}(z) & A_{22}(z) & \cdots & A_{2m}(z) \\ \vdots & & \ddots & \\ A_{m1}(z) & A_{m2}(z) & \cdots & A_{mm}(z) \end{bmatrix}; \mathbf{X}(n) = \begin{bmatrix} X_1(n) \\ X_2(n) \\ \vdots \\ X_m(n) \end{bmatrix}; \mathbf{W}(n) = \begin{bmatrix} W_1(n) \\ W_2(n) \\ \vdots \\ W_m(n) \end{bmatrix}; \quad \text{(A.1)}$$

the multivariate dependencies can be rewritten as

$$\begin{aligned} \mathbf{X}(z) &= -\mathbf{A}(z)\mathbf{X}(z) + \mathbf{W}(z) \Leftrightarrow \\ (I_m + \mathbf{A}(z))\mathbf{X}(z) &= \mathbf{W}(z) \Leftrightarrow \\ \mathbf{X}(z) &= (I_m + \mathbf{A}(z))^{-1}\mathbf{W}(z) \Leftrightarrow \\ \\ \Rightarrow \mathbf{H}(z) &= (I_m + \mathbf{A}(z))^{-1} \end{aligned} \quad \text{(A.2)}$$

where $\mathbf{X}(z)$ and $\mathbf{W}(z)$ are the $z$-transform of $\mathbf{X}(n)$ and $\mathbf{W}(n)$ and $I_m$ is the $m \times m$ identity matrix. In (A.2), the matrix that results as the inverse of the coefficient matrix $(I_m + \mathbf{A}(z))$, assumes the form

$$\mathbf{H}(z) = \begin{bmatrix} H_{11}(z) & H_{12}(z) & \cdots & H_{1m}(z) \\ H_{21}(z) & H_{22}(z) & \cdots & H_{2m}(z) \\ \vdots & & \ddots & \\ H_{m1}(z) & H_{m2}(z) & \cdots & H_{mm}(z) \end{bmatrix} \quad \text{(A.3)}$$

and it is the closed-loop transfer functions matrix. Each $(i, l)$ element in (A.3) is a complex-valued function of $z$ expressing the relationship between the time series $X_i$ and $X_l$.

The coefficients of the polynomials $\mathbf{A}(z)$ can be estimated using a least squares approach and implemented in *Matlab* using the facilities of the *System Identification Toolbox*.

**Model order selection**

For simplicity, the same order $p$ is assumed for all AR polynomials. Since models order $p$ is not known a priori, in order to obtain the optimum $p$ value, the polynomial coefficients are estimated up to a chosen maximum order and the optimum order is selected according to the Akaike Information Criterion (AIC) (Waele and Broersen, 2003). This order selection criterion is based on the determinant of the estimated covariance matrix ($\hat{\mathbf{\Sigma}}$) of the generating white noises of the estimated AR($p$) model plus a penalty factor for the number of estimated parameters ($m^2p$)

$$AIC(p) = N \ln(\det \hat{\mathbf{\Sigma}}) + 2m^2p \tag{A.4}$$

The number of estimated parameters should be less than 10% with respect to the total number of observations, in order to reduce overfit problems.

## A.2 Spectral parameters

The autoregressive multivariate identification is able to compute classical cross-spectral parameters, such as the spectra and the cross-spectra matrix $\mathbf{S}(f)$, as

$$\begin{aligned} \mathbf{S}(f) &= 2\pi S(\Omega) = 2\pi T_X I_m \mathbf{S}(z)|_{z=e^{j\Omega T_X}} \\ \mathbf{S}(z) &= \mathbf{H}(z)\mathbf{\Sigma}\mathbf{H}^T(z^{-1}), \end{aligned} \tag{A.5}$$

where $\Omega = 2\pi f$ with $f$ the frequency in Hz, $\mathbf{H}(z)$ is the transfer functions matrix, $\mathbf{\Sigma}$ is the covariance matrix of the noise sources and $T_X$ is the sampling period of the time series $X_i$, $i = 1, 2, ...m$. The complex spectral matrix $\mathbf{S}(z)$ assumes the form

$$\mathbf{S}(z) = \begin{bmatrix} S_{11}(z) & S_{12}(z) & \cdots & S_{1m}(z) \\ S_{21}(z) & S_{22}(z) & \cdots & S_{2m}(z) \\ \vdots & & \ddots & \\ S_{m1}(z) & S_{m2}(z) & \cdots & S_{mm}(z) \end{bmatrix}, \tag{A.6}$$

where each $S_{ii}(z)$ is the complex spectrum of the time series $X_i$. As the noises are assumed to be uncorrelated, $\mathbf{\Sigma}$ can be approximated as a diagonal matrix

$$\mathbf{\Sigma} \cong \begin{bmatrix} \lambda_1^2 & 0 & \cdots & 0 \\ 0 & \lambda_2^2 & & 0 \\ \vdots & & \ddots & \vdots \\ 0 & 0 & \cdots & \lambda_m^2 \end{bmatrix} \tag{A.7}$$

and, from (A.5), $S_{ii}(z)$ can be written as

$$\begin{aligned} S_{ii}(z) &= H_{i1}(z)\lambda_1^2 H_{i1}(z^{-1}) + \cdots + H_{im}(z)\lambda_m^2 H_{im}(z^{-1}) \\ &= \sum_{k=1}^{m} H_{ik}(z)\lambda_k^2 H_{ik}(z^{-1}) = \sum_{k=1}^{m} SP_{ii}^{(k)}(z) \end{aligned} \tag{A.8}$$

that is, $S_{ii}(z)$ can be seen as the sum of partial complex spectra $SP_{ii}^{(k)}(z)$, each one representing the contribution from the respective input noise.

Also, the degree of linear correlation between two signals $X_i$ and $X_l$ as a function of the frequency $f$ can be expressed through the coherence function or the magnitude squared coherence

$$|k_{il}(f)|^2 = \frac{|S_{il}(f)|^2}{S_{ii}(f)S_{ll}(f)}. \tag{A.9}$$

## A.3 Parametric decomposition

To every spectral density (or partial spectra) is associated a transfer function $H(z)$. From the roots of $H(z)$, it is possible to factorize or decompose the spectral density in $p$ components, referred to each pole. The decomposition here presented was achieved in an independent way and is concordant with Johnsen and Andersen (1978) and Baselli *et al.* (1997).

The transfer function of an ARMA$_{p,q}$ model is given by

$$H(z) = \frac{b_0 + b_1 z^{-1} + ... + b_q z^{-q}}{1 + a_1 z^{-1} + ... + a_p z^{-p}} = \frac{B(z)}{A(z)} = \frac{B(z)}{\prod_{k=1}^{p}(z - z_k)},\ p > q \tag{A.10}$$

and $z_k$, $k = 1, ..., p$ are the poles of $H(z)$. For a sampling period $T$ and a variance of the source noise $\lambda^2$ , the spectrum can be written as

$$\begin{aligned} S(f) &= 2\pi S(\Omega) = 2\pi T S(z)|_{z=e^{j\Omega T}} \\ S(z) &= H(z)\lambda^2 H(z^{-1}), \end{aligned} \tag{A.11}$$

where $\Omega = 2\pi f$ with $f$ the frequency in Hz. By definition, the complex spectrum $S(z)$ can be obtained from the autocorrelation function $R(\tau)$ as

$$S(z) = \sum_{\tau=-\infty}^{+\infty} R(\tau) z^{-\tau}. \tag{A.12}$$

Inverting the Z-transform,

$$\begin{aligned} R(\tau) &= \frac{1}{2\pi j} \oint_{|z|=1} S(z) z^{\tau-1}, \tau = 0, 1, 2, ... \\ R(-\tau) &= R(\tau) \end{aligned}$$

and computing the line integral using the *Cauchy Residue Theorem*, we can write the autocorrelation function $R(\tau)$ as

$$\begin{aligned} R(\tau) &= \sum_{k=1}^{p} R_k(\tau), \\ R_k(\tau) &= \left( \text{Res} \left[ \frac{S(z)}{z} \right]_{z=z_k} \right) z_k^{\tau} = \gamma_k z_k^{\tau} \end{aligned}$$

The residue $\gamma_k$ can be computed and simplified using equations (A.10) and (A.11)

$$\gamma_k = \frac{B(z_k)\lambda^2 B(z_k^{-1})}{\prod_{\substack{h=1 \\ h \neq k}}^{p} (z_k - z_h) \prod_{h=1}^{p} (z_k^{-1} - z_h) z_k}.$$

By the linearity of the bilateral Z-transform, from equation (A.12) is obtained

$$\begin{aligned} S(z) &= \sum_{k=1}^{p} S^{(k)}(z) \\ S^{(k)}(z) &= \frac{\gamma_k z_k}{(z^{-1} - z_k)} + \gamma_k + \frac{\gamma_k z_k}{(z - z_k)}. \end{aligned} \tag{A.13}$$

In this way, the complex spectrum $S(z)$ in (A.11) can be decomposed into $p$ components $S^{(k)}(z)$, each one referred to the pole $z_k$.

Considering the equivalent decomposition of the power spectrum $S(f)$ in (A.11), components $S^{(k)}(f)$ are obtained for each $f_k = arg(z_k)/(2\pi T)$. At lag $\tau = 0$, $R(0)$ represents the total variance (or power) in the spectrum $S(f)$, and by (A.13), the following relation is established

$$R(0) = \sum_{k=1}^{p} R_k(0) = \sum_{k=1}^{p} \gamma_k. \tag{A.14}$$

that is, $\gamma_k$ can be interpreted as the contribution in $R(0)$ related with the component $S^{(k)}(f)$. To a frequency $f_k = 0$ or $f_k = 1/2T$ (that is, for $z_k$ real) corresponds a real component with power $\gamma_k$. As frequencies $f_k$ and $-f_k$ are associated to complex conjugate poles (and therefore, complex conjugate components), a single real component is considered as the sum of the correspondent $S^{(k)}(z)$ and its conjugate, with power $\gamma_k + \gamma_k^* = 2\Re(\gamma_k)$. In this way, the power of the component $S^{(k)}(f)$ can be obtained from $\gamma_k$.

The power within a given frequency band $B$ (Hz) can be estimated by summing the contributions of the poles with frequency $f_k$ located in $B$, that is

$$\hat{P}^B = \sum_{f_k \in B} c_k \, \Re(\gamma_k), \tag{A.15}$$

where $c_k = 1$ for real poles and $c_k = 2$ for complex conjugate poles.

This algebraic decomposition of the spectrum does not guaranty the achievement of admissible spectral components, once negative estimates of $S^{(k)}(f)$ power can occur, if poles are too close together (Marple, 1987). If this happens near the limit of a frequency band $B$, a negative $\hat{P}^B$ value can be obtained.

# Appendix B

# Sequences technique and outlier effect

## B.1 Least squares generalities

Consider $(x_k, y_k)$, $k = 1, 2, ..., n$ observations of a given phenomena. Assuming the linear model $y = \alpha x + \beta$, the least squares estimates of the parameters $\alpha$ and $\beta$ can be computed by minimizing the sum of the deviation squares as

$$R = \sum_{k=1}^{n} \left[ y_k - \left( \hat{\alpha} x_k + \hat{\beta} \right) \right]^2 \tag{B.1}$$

Taking the partial derivatives of $R$ with respect to the variables $\alpha$ and $\beta$, setting each one equal to zero and solving the resulting system of two equations with the two unknowns, yiels the following estimators for the parameters

$$\hat{\alpha} = \frac{\sum_{k=1}^{n} (x_k - \bar{x})(y_k - \bar{y})}{\sum_{k=1}^{n} (x_k - \bar{x})^2}; \; \hat{\beta} = \bar{y} - \hat{\alpha}\bar{x};$$

## B.2 Sequences technique: the local approach

Let $(x, y)$ be a baroreflex sequence and $(x, y)_{(i,k)}$ the $k$-th value of the $i$-th baroreflex sequence, such as $k = 1, 2, 3$ and $i = 1, 2, ..., n$, without loss of generality.

For a baroreflex sequence of length 3, the local baroreflex gain of the $i$-th baroreflex sequence, $G_l^{(i)}$, is estimated as the slope of the best line in least squares sense or

$$G_l^{(i)} = \frac{\sum_{k=1}^{3}(x_{(i,k)} - \bar{x}_{(i)})(y_{(i,k)} - \bar{y}_{(i)})}{\sum_{k=1}^{3}(x_{(i,k)} - \bar{x}_{(i)})^2}$$

and, an overall estimate $G_{local}$ can be obtained from the mean of the $n$ local gains

$$G_{local} = \frac{1}{n}\sum_{k=1}^{n} G_l^{(k)}$$

Inserting a perturbation $\epsilon > 0$ in the $j$-th value of the $i$-th baroreflex sequence, let it be the $\hat{y}_{(i,j)} = y_{(i,j)} + \epsilon$, the local baroreflex perturbed gain $G_{lp}^{(i)}$ gain is now

$$G_{lp}^{(i)} = \frac{\sum_{k=1}^{3}(x_{(i,k)} - \bar{x}_{(i)})(\hat{y}_{(i,k)} - \hat{\bar{y}}_{(i)})}{\sum_{k=1}^{3}(x_{(i,k)} - \bar{x}_{(i)})^2}$$

where $\hat{\bar{y}}_{(i)}$, the mean value of the values $\hat{y}_{(i,k)}$, $k = 1, 2, 3$, is given by

$$\hat{\bar{y}}_{(i)} = \frac{1}{3}\sum_{k=1}^{3}\hat{y}_{(i,k)} = \frac{1}{3}\left(\sum_{\substack{k=1\\k\neq j}}^{3} y_{(i,k)} + \hat{y}_{(i,j)}\right) = \bar{y}_{(i)} + \frac{\epsilon}{3}$$

Therefore, $G_{lp}^{(i)}$ assumes the form

$$G_{lp}^{(i)} = \frac{\sum_{\substack{k=1\\k\neq j}}^{3}(x_{(i,k)} - \bar{x}_{(i)})(y_{(i,k)} - \hat{\bar{y}}_{(i)}) + (x_{(i,j)} - \bar{x}_{(i)})(\hat{y}_{(i,j)} - \hat{\bar{y}}_{(i)})}{\sum_{k=1}^{3}(x_{(i,k)} - \bar{x}_{(i)})^2} =$$

$$= G_l^{(i)} + \frac{-\frac{\epsilon}{3}\sum_{k=1}^{3}(x_{(i,k)} - \bar{x}_{(i)}) + \epsilon(x_{(i,j)} - \bar{x}_{(i)})}{\sum_{k=1}^{3}(x_{(i,k)} - \bar{x}_{(i)})^2} = G_l^{(i)} + \epsilon_l^{(i)}$$

with $\epsilon_l^{(i)}$ the perturbation in the baroreflex gain introduced by the $j$-th value in the $i$-th sequence.

The overall estimate $G_{local}^{(p)}$ is

$$G_{local}^{(p)} = \frac{1}{n}\left(\sum_{\substack{k=1\\k\neq i}}^{n} G_l^{(k)} + G_{lp}^{(i)}\right) \quad = \frac{1}{n}\left(\sum_{k=1}^{n} G_l^{(k)} + \epsilon_l^{(i)}\right) = G_{local} + \frac{1}{n}\epsilon_l^{(i)}$$

Thus, the error introduced in local approach by the perturbation $\epsilon$ is

$$E_{local}^{(p)} = \frac{1}{n}\frac{-\frac{\epsilon}{3}\sum_{k=1}^{3}(x_{(i,k)} - \bar{x}_{(i)}) + \epsilon(x_{(i,j)} - \bar{x}_{(i)})}{\sum_{k=1}^{3}(x_{(i,k)} - \bar{x}_{(i)})^2}$$

## B.3 Sequences technique: the global approach

Let $(x, y)$ be a baroreflex sequence and $(x, y)_{(i,k)}$ the $k$-th value of the $i$-th baroreflex sequence, such as $k = 1, 2, 3$ and $i = 1, 2, ..., n$, without loss of generality. For a baroreflex sequence of length 3, the global baroreflex gain is estimated as the slope of the best line in least squares sense that better adjusts all $(x, y)$ sequences or

$$G_{global} = \frac{\sum_{l=1}^{n}\sum_{k=1}^{3}(x_{(l,k)} - \bar{x})(y_{(l,k)} - \bar{y})}{\sum_{l=1}^{n}\sum_{k=1}^{3}(x_{(l,k)} - \bar{x})^2}$$

where $\bar{x}$ and $\bar{y}$ represent the global mean of variables $x$ and $y$. Inserting a perturbation $\epsilon > 0$ in the $j$-th value of the $i$-th baroreflex sequence, let it be the $\hat{y}_{(i,j)} = y_{(i,j)} + \epsilon$, the global baroreflex perturbed gain $G_{global}^{(p)}$ gain is now

$$G_{global}^{(p)} = \frac{\sum_{l=1}^{n}\sum_{k=1}^{3}(x_{(l,k)} - \bar{x})(\hat{y}_{(l,k)} - \hat{\bar{y}})}{\sum_{l=1}^{n}\sum_{k=1}^{3}(x_{(l,k)} - \bar{x})^2}$$

where $\hat{\bar{y}}$, the mean value of the new samples, is

$$\hat{\bar{y}} = \frac{1}{3n}\sum_{i=1}^{3n}\hat{y}_{(i)} = \frac{1}{n}\left(\sum_{\substack{l=1\\l\neq i}}^{n}\left(\frac{1}{3}\sum_{k=1}^{3}y_{(l,k)}\right) + \frac{1}{3}\sum_{k=1}^{3}\hat{y}_{(i,k)}\right) = \frac{1}{n}\sum_{l=1}^{n}\left(\frac{1}{3}\sum_{k=1}^{3}y_{(l,k)}\right) + \frac{\epsilon}{3n}$$
$$= \hat{y} + \frac{\epsilon}{3n}$$

Therefore, the $G^{(p)}_{global}$ is given by

$$G^{(p)}_{global} = \frac{\sum_{\substack{l=1\\l\neq i}}^{n}\sum_{k=1}^{3}(x_{(l,k)}-\bar{x})(y_{(l,k)}-\hat{\bar{y}}) + \sum_{\substack{k=1\\k\neq j}}^{3}(x_{(i,k)}-\bar{x})(y_{(i,k)}-\hat{\bar{y}}) + (x_{(i,j)}-\bar{x})(\hat{y}_{(i,j)}-\hat{\bar{y}})}{\sum_{l=1}^{n}\sum_{k=1}^{3}(x_{(l,k)}-\bar{x})^2} =$$
$$= G_{global} + \frac{-\frac{\epsilon}{3n}\sum_{l=1}^{n}\sum_{k=1}^{3}(x_{(l,k)}-\bar{x}) + \epsilon(x_{(i,j)}-\bar{x})}{\sum_{l=1}^{n}\sum_{k=1}^{3}(x_{(l,k)}-\bar{x})^2}$$

Thus, the error introduced in global approach by the perturbation $\epsilon$ is

$$E^{(p)}_{global} = \frac{-\frac{\epsilon}{3n}\sum_{l=1}^{n}\sum_{k=1}^{3}(x_{(l,k)}-\bar{x}) + \epsilon(x_{(i,j)}-\bar{x})}{\sum_{l=1}^{n}\sum_{k=1}^{3}(x_{(l,k)}-\bar{x})^2}$$